World Journal of Clinical Oncology

Submit a Manuscript: https://www.f6publishing.com

World J Clin Oncol 2023 October 24; 14(10): 373-399

DOI: 10.5306/wjco.v14.i10.373

ISSN 2218-4333 (online)

ORIGINAL ARTICLE

Basic Study

Comprehensive analysis of disulfidptosis related genes and prognosis of gastric cancer

Qian Li, Long-Kuan Yin

Specialty type: Oncology

Provenance and peer review: Unsolicited article; Externally peer reviewed.

Peer-review model: Single blind

Peer-review report's scientific quality classification

Grade A (Excellent): 0
Grade B (Very good): B, B
Grade C (Good): 0
Grade D (Fair): 0
Grade E (Poor): 0

P-Reviewer: Ozturk E, Turkey; Rhoden CRB, Brazil

Received: July 30, 2023
Peer-review started: July 30, 2023
First decision: August 24, 2023
Revised: September 7, 2023
Accepted: September 18, 2023
Article in press: September 18, 2023
Published online: October 24, 2023

Qian Li, Department of Oncology, Fushun Hospital of Traditional Chinese Medicine, Zigong 643200, Sichuan Province, China

Long-Kuan Yin, Department of Gastrointestinal Surgery, Fushun People's Hospital, Zigong 643200, Sichuan Province, China

Corresponding author: Long-Kuan Yin, Doctor, Researcher, Department of Gastrointestinal Surgery, Fushun People's Hospital, No. 490 Jixiang Road, Fushi Town, Zigong 643200, Sichuan Province, China. 782286066@qq.com

Abstract

BACKGROUND

Gastric cancer (GC) is a common malignant tumor of the digestive system. Disulfidptosis is a new programmed cell death mechanism, although its specific mechanism in GC is incompletely understood.

AIM

In this study, we used bioinformatics analysis to explore a disulfidptosis-based predictive model related to GC prognosis and to identify potential therapeutic targets and sensitive drugs for GC.

METHODS

We extracted GC-related data from The Cancer Genome Atlas and Gene Expression Omnibus databases. R software (version 4.2.1) was used for correlation analysis.

RESULTS

Through the above analysis, we found that the disulfidptosis related gene may be related to the prognosis of GC. Six genes, namely, *PLS3*, *GRP*, *APOD*, *SGCE*, *COL8A1*, and *VAMP7*, were found to constitute a predictive model for GC prognosis. *APOD* is a potential therapeutic target for treating GC. Bosutinib and other drugs are sensitive for the treatment of GC.

CONCLUSION

The results of this study indicate that disulfidptosis is related to the prognosis and treatment of GC, while *APOD* represents a potential therapeutic target for GC.

Key Words: Gastric cancer; Disulfidptosis; Drugs; Prognosis; Targets

Core Tip: Gastric cancer (GC) is a common malignant tumor of the digestive system. Disulfidptosis is a new programmed cell death mechanism. The specific mechanism of disulfidptosis in GC is not fully understood. This study found that the disulfidptosis related gene may be related to the prognosis of gastric cancer. *PLS3*, *GRP*, *APOD*, *SGCE*, *COL8A1*, *VAMP7*, these six genes constitute a predictive model for gastric cancer prognosis. *APOD* is a potential therapeutic target. Bosutinib and other drugs are sensitive for the treatment of gastric cancer.

Citation: Li Q, Yin LK. Comprehensive analysis of disulfidptosis related genes and prognosis of gastric cancer. *World J Clin Oncol* 2023; 14(10): 373-399
URL: https://www.wjgnet.com/2218-4333/full/v14/i10/373.htm
DOI: https://dx.doi.org/10.5306/wjco.v14.i10.373

INTRODUCTION

Gastric cancer (GC) is a common cause of cancer-related death worldwide, with a particularly high incidence in East Asia, such as South Korea, China, and Japan[1-9]. The early clinical symptoms of GC are not obvious and lack specificity[10-14], which leads to a low rate of early diagnosis[15-26]. Most patients with GC are diagnosed late and have a poor prognosis[27-40]. Although the diagnosis and treatment strategies for GC have gradually increased in recent decades, the prognosis of advanced GC remains poor[41-47]. Therefore, there is an urgent need to find more biomarkers as novel therapeutic targets and to develop new drugs to improve diagnosis and treatment measures and, consequently, patient survival and prognosis.

GC is a heterogeneous disease[48], with previous studies suggesting that various cell programmed death mechanisms, including ferroptosis[49-54] and cuproptosis[55-58], represent novel research directions for GC. In recent years, it has been found that disulfidptosis[59], a novel and poorly studied mechanism of programmed cell death, represents a previously uncharacterized form of cell death induced by abnormal accumulation of disulfide in cells under glucose starvation, which is different from copper death and iron death. However, its role in GC and its related mechanisms are still unclear and need to be further explored.

In this study, we analyzed the sequencing data of tumor tissues from databases such as The Cancer Genome Atlas (TCGA)[60] and Gene Expression Omnibus (GEO) (Supplementary material)[61] and 14 disulfidptosis-related gene (DRGs)[59] (*ACTN4, ACTB, CD2AP, CAPZB, DSTN, FLNA, FLNB, INF2, IQGAP1, MYH10, MYL6, MYH9, PDLIM1,* and *TLN1*). We conducted differential analysis of DRGs, as well as analyses of the tumor mutation burden (TMB)[62,63], copy variations, gene ontology (GO)[64], and the kyoto encyclopedia of genes and genomes (KEGG)[65], among others. In this paper, the mechanism of DRGs involved in the occurrence and development of GC is discussed, and new therapeutic targets and drugs that may be related to the prognosis of GC are preliminarily analyzed and screened from a new perspective.

MATERIALS AND METHODS

Data downloading and processing

Expression data, clinical data, mutation data, and copy data related to GC were downloaded and organized from TCGA database. The GSE84433 and GSE26253 datasets and their platform annotation files were downloaded from the GEO database. Data were analyzed and processed using R software (version 4.2.1) and Perl software (version 5.30.0).

Differential and prognostic analyses

GC-related data were extracted from TCGA database and analyzed in combination with the disulfidptosis-related gene. Differential analysis, mutation load analysis, copy number variation frequency analysis, and survival analysis were performed using R software.

Disulfidptosis subtype analysis

R software was used to classify all samples related to the disulfidptosis-related gene in TCGA and GEO databases for survival analysis, heatmap clustering, gene set variation analysis (GSVA), immune cell differential analysis, subtype differential analysis, and GO and KEGG enrichment analyses.

Significant differential gene subtyping, prediction model construction, and analysis

We continued to perform survival analysis, heatmap clustering, and differential analysis of the DRGs on the samples classified by differential gene subtyping. Then, we randomly divided the significant differential samples into groups and performed least absolute shrinkage and selection operator (LASSO) regression analysis and univariate and multivariate

Cox regression analyses and constructed a prognostic model. Using the prognostic model, we calculated the risk score for each patient sample using the following formula:.where $Coef_i$ is the coefficient, and X_i is the expression level of the gene. We constructed a prognostic evaluation model for overall survival based on the risk score. We then constructed a Sankey diagram and analyzed the differences in risk scores between subtypes and the differential risk of the DRGs.

Prognostic model validation

The reliability of the prognostic model was verified by survival analysis, receiver operating characteristic (ROC) curve mapping, risk curve mapping, survival state map, and clustering heatmap of model genes in each subgroup.

Nomogram construction and analysis of the correlation between risk score and immunity, as well as drug susceptibility

Next, the independent prognostic factors of GC and potential therapeutic targets were sought by constructing the column diagram, and survival analysis of potential prognostic genes was performed by Gene Expression Profiling Interactive Analysis (GEPIA). Subsequently, immune cell correlation analysis, tumor microenvironment (TME) difference analysis, waterfall map construction, tumor mutation load analysis, microsatellite instability (MSI), stem cell correlation analysis, and drug sensitivity analysis were performed for the risk score.

Immunohistochemical analysis

We conducted immunohistochemical analysis of *APOD* using the human protein atlas (HPA) network database, comparing the differences in protein expression between GC tissues and adjacent normal tissues.

Statistical analysis

All statistical analyses were performed using R software (version 4.2.1). A P-value < 0.05 was considered statistically significant.

RESULTS

Difference analysis and prognosis analysis of DRGs

Difference analysis revealed that 10 DRGs, namely, *ACTN4*, *ACTB*, *CD2AP*, *CAPZB*, *FLNB*, *INF2*, *IQGAP1*, *MYH10*, *MYH9* and *PDLIM1*, were significantly different in GC samples and adjacent normal tissue samples (Figure 1A). Through mutation load analysis, copy number variation frequency analysis, and a genosphere map, we found that *CAPZB* and *MYL6* were not mutated, while *MYH10* had the most mutations. It was also found that *CAPZB* had the most deletion mutations, while *IQGAP1* had the most insertion mutations. Cyclic analysis led to the identification of disulfidptosis mutations in 14 chromosomes (Figure 1B-D). Moreover, survival analysis showed that patients with high expression of *TLN1*, *MYL6*, *MYH10*, *MYH9*, *IQGAP1*, *INF2*, *FLNA*, *DSTN*, and *ACTB* had a reduced survival time, while those with high expression of *PDLIM1* had an increased survival time (Figure 2A–J). Prognostic network diagram analysis showed that disulfidptosis-related genes, including *PDLIM1*, *FLNA*, *MYH10*, *MYL6*, and *DSTN*, were significantly correlated with the prognosis of GC (P < 0.05), and *DSTN*, *FLNA*, *MYH10*, and *MYL6* were risk factors for the prognosis of GC, while *PDLIM1* was a favorable factor for the prognosis of GC (Figure 2K).

Subtyping of the DRGs and analysis through GSVA, single-sample gene set enrichment analysis, GO, and KEGG analyses

Through clustering analysis of the DRG samples, we found that the best way to divide the samples was into two subtypes, A and B (Figure 3A-D). Through survival analysis of the two subtypes, we found significant differences between the groups, P < 0.05 (Figure 3E), and through clustering heatmap analysis, we found that most DRGs were upregulated in cluster A and downregulated in cluster B (Figure 3F). Using the GSVA package in R software, we performed KEGG pathway enrichment analysis on the DRG subtyping samples and found that the significantly different pathways enriched in the two subtypes included glutamate and glutamine metabolism, extracellular matrix receptor interaction, the transforming growth factor-beta (TGF-β) signaling pathway, and the pentose phosphate pathway (Figure 4A). Through GO functional enrichment analysis of the DRG subtyping samples with the GSVA package in R, we found that the main enrichment was in the positive regulation of the transforming growth factor receptor and Wnt signaling pathways (Figure 4B). We also found significant differences in immune cells, such as activated CD4 T cells, and activated CD8 T cells, between subtypes A and B, according to the analysis of the differences in immune cells between the subtypes (Figure 5A). Subtype differential analysis led to the identification of 282 significantly different co-expressed genes between subtypes A and B (Figure 5B and C). Moreover, GO analysis of these differentially expressed genes revealed that the enriched functions of these differentially expressed genes were mainly in the extracellular matrix tissue and negative regulation of the typical Wnt signaling pathway (Figure 5D). KEGG analysis of these differentially expressed genes revealed that these genes were enriched in the TGF-β, Wnt, and MAPK signaling pathways, as well as in other pathways (Figure 5E).

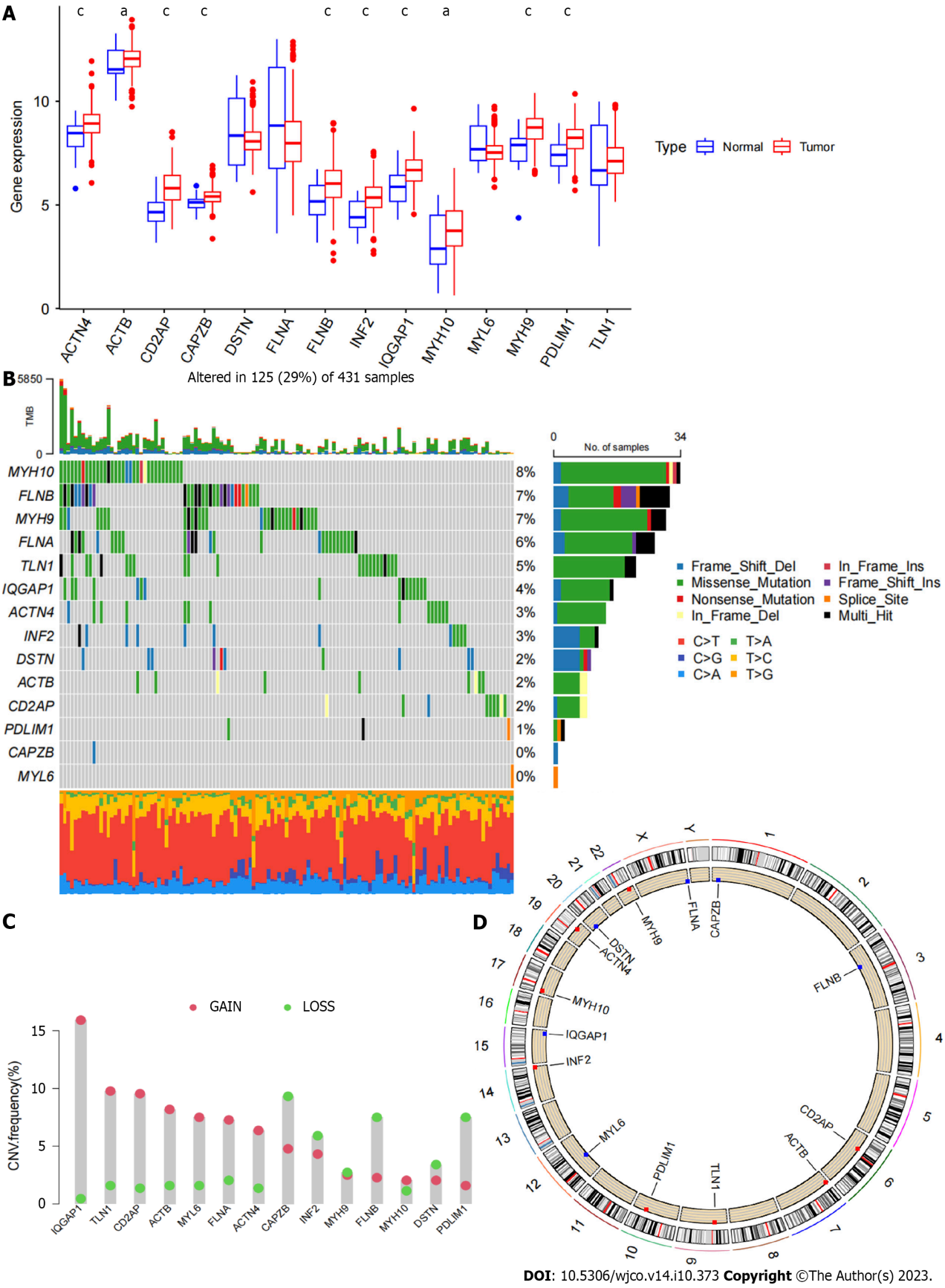

DOI: 10.5306/wjco.v14.i10.373

Figure 1 The results of the differential expression analysis of disulfidptosis related genes in gastric cancer and adjacent normal tissues are presented. A: Shows the difference analysis of disulfidptosis related genes in gastric cancer tissue samples and adjacent normal tissue samples; B: Shows the waterfall plot of disulfidptosis related genes mutations; C: Presents the mutation frequency of disulfidptosis related genes; D: Shows the mutation sites of disulfidptosis related genes. CNV: Copy number variation.

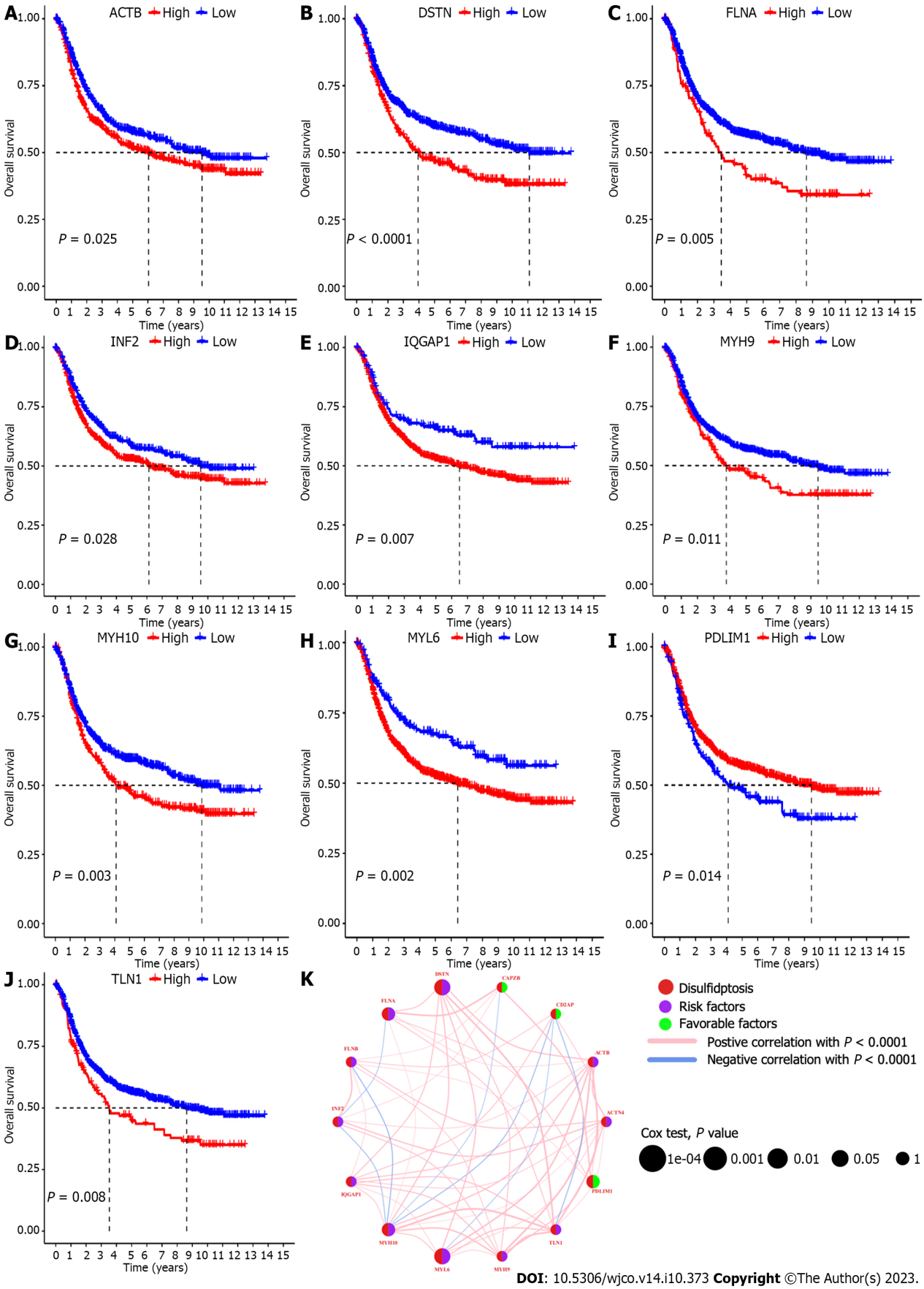

DOI: 10.5306/wjco.v14.i10.373

Figure 2 Screening disulfidptosis related genes related to the prognosis of gastric cancer. A-J: Show the Kaplan-Meier analysis of the survival curves of disulfidptosis related genes between high and low expression groups, and 10 disulfidptosis related genes related to gastric cancer prognosis were identified; K: Shows the COX analysis of the disulfidptosis related genes circle plot related to gastric cancer prognosis, and five significantly prognostic disulfidptosis related genes were identified.

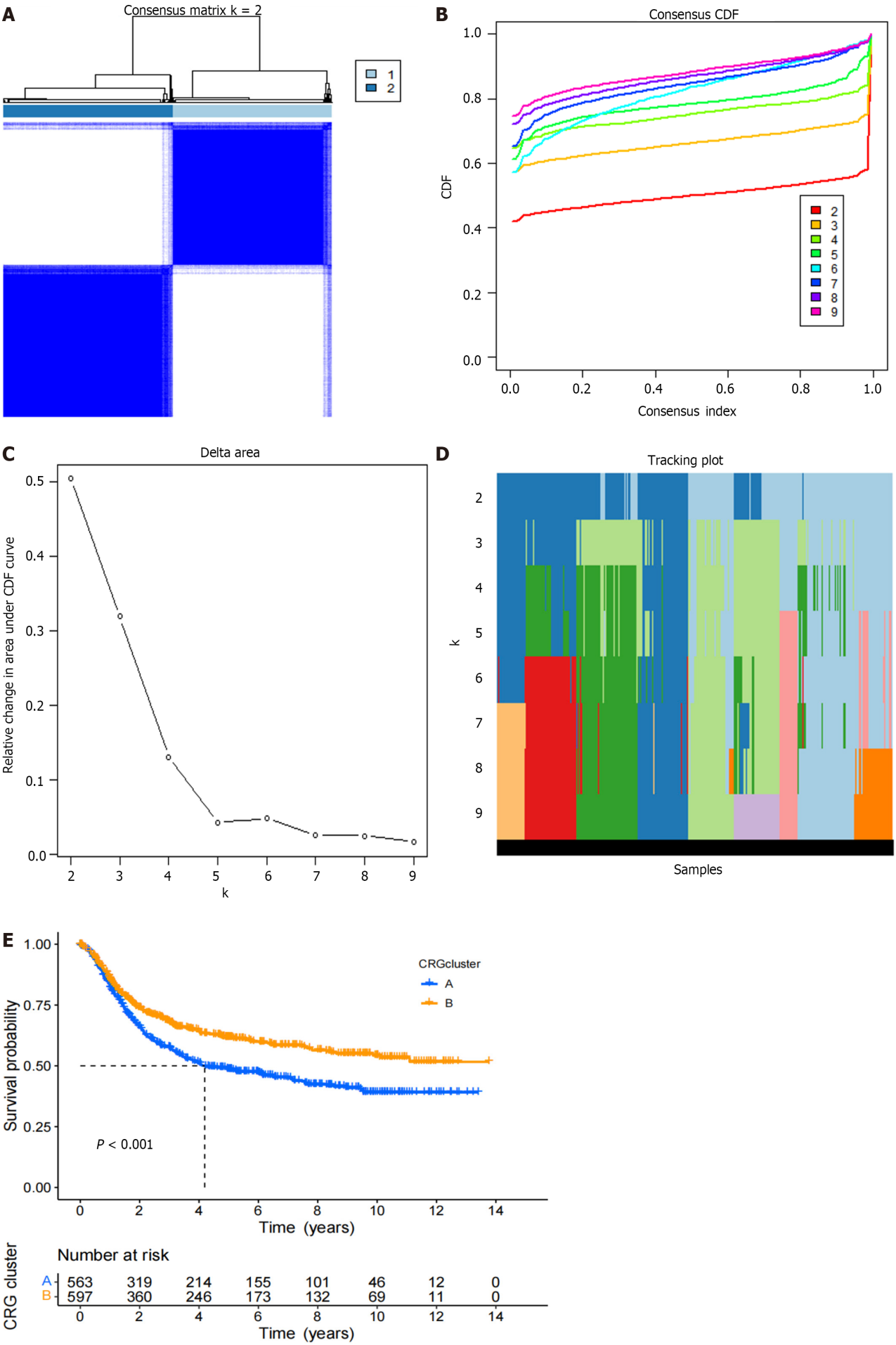
A
Consensus matrix k = 2
1
2
B
Consensus CDF
CDF
Consensus index
2
3
4
5
6
7
8
9
C
Delta area
Relative change in area under CDF curve
k
D
Tracking plot
k
Samples
E
CRGcluster
A
B
Survival probability
P < 0.001
Time (years)
Number at risk
CRG cluster
A 563 319 214 155 101 46 12 0
B 597 360 246 173 132 69 11 0
Time (years)

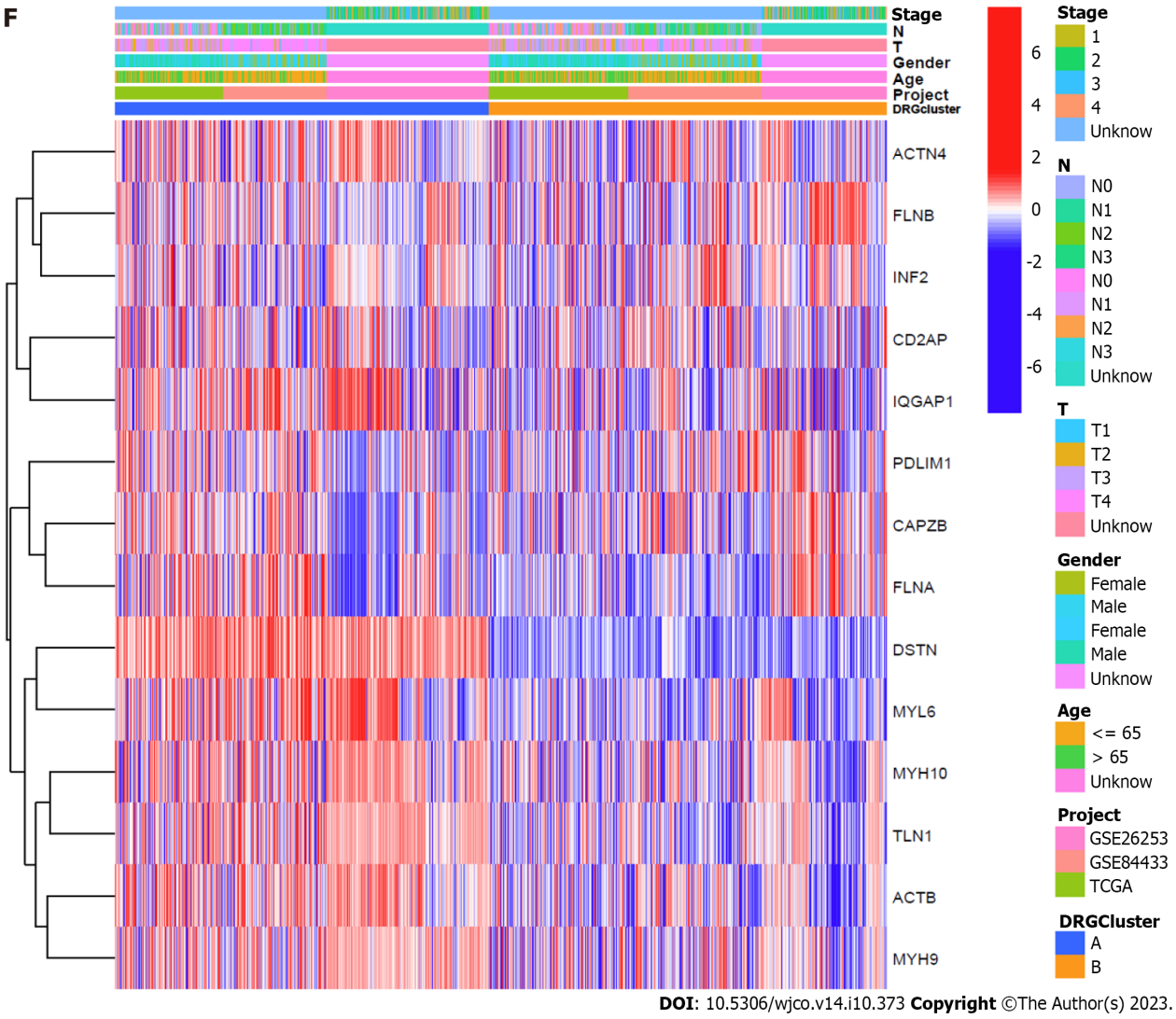

DOI: 10.5306/wjco.v14.i10.373

Figure 3 The sample classification, subgroup survival analysis, and differential gene heatmap related to disulfidptosis related genes are presented. A: Shows the clustering matrix plot of disulfidptosis related genes-related samples; B: Shows the clustering index plot of disulfidptosis related genes-related samples; C: Presents the relative change area under the cumulative distribution function curve; D: Shows the tracking plot of disulfidptosis related genes subgroup samples; E: Presents the survival analysis curves of disulfidptosis related genes subgroups; F: Shows the differential gene clustering heatmap between disulfidptosis related genes subgroups.

Classification and correlation analysis of significant differentially expressed genes obtained from the disulfidptosis subtype samples

The related samples of differentially expressed genes were clustered into three subtypes (Figure 6A–D). Survival analysis showed that the prognosis of subtype C was different from that of subtypes A and B, with better prognosis for subtypes B and C (Figure 6E). Heatmap analysis showed that most samples in subtype C were upregulated, while most samples in subtype B were downregulated (Figure 6F). Differential expression analysis of the DRGs in the different gene subtypes showed that the expression of the DRGs was different in subtypes A, B, and C, with $P < 0.05$ (Figure 6G). We used the create data partition package to randomly divide the samples into two groups of equal size, the training and testing groups. Then, using LASSO regression and Cox regression, we analyzed the training group samples and constructed a six-gene risk model based on the DRG subtype: Risk score = (0.164102181511909* *PLS3* expression) + (0.079055019007862* *GRP* expression) + (0.0649967121599996* *APOD* expression) + (0.0920219139298833* *SGCE* expression) + (0.107438278125729* *COL8A1* expression) + (–0.0723643090076661* *VAMP7* expression) (Figure 6H and I). The results of the risk model are shown in Supplementary Table 1. The Sankey diagram shows the distribution of samples among the different groups (Figure 7A). By evaluating the risk score for each group, we found significant differences in the risk between the groups (Figure 7B and C). By evaluating the risk score for the DRGs, we found that the expression levels of 13 DRGs differed significantly between the high and low risk groups, with nine genes showing higher expression in the high-risk group and four genes showing higher expression in the low-risk group (Figure 7D).

Validation results of the risk model

We next used the risk model to score the differential gene-related samples mentioned above and then divided them into

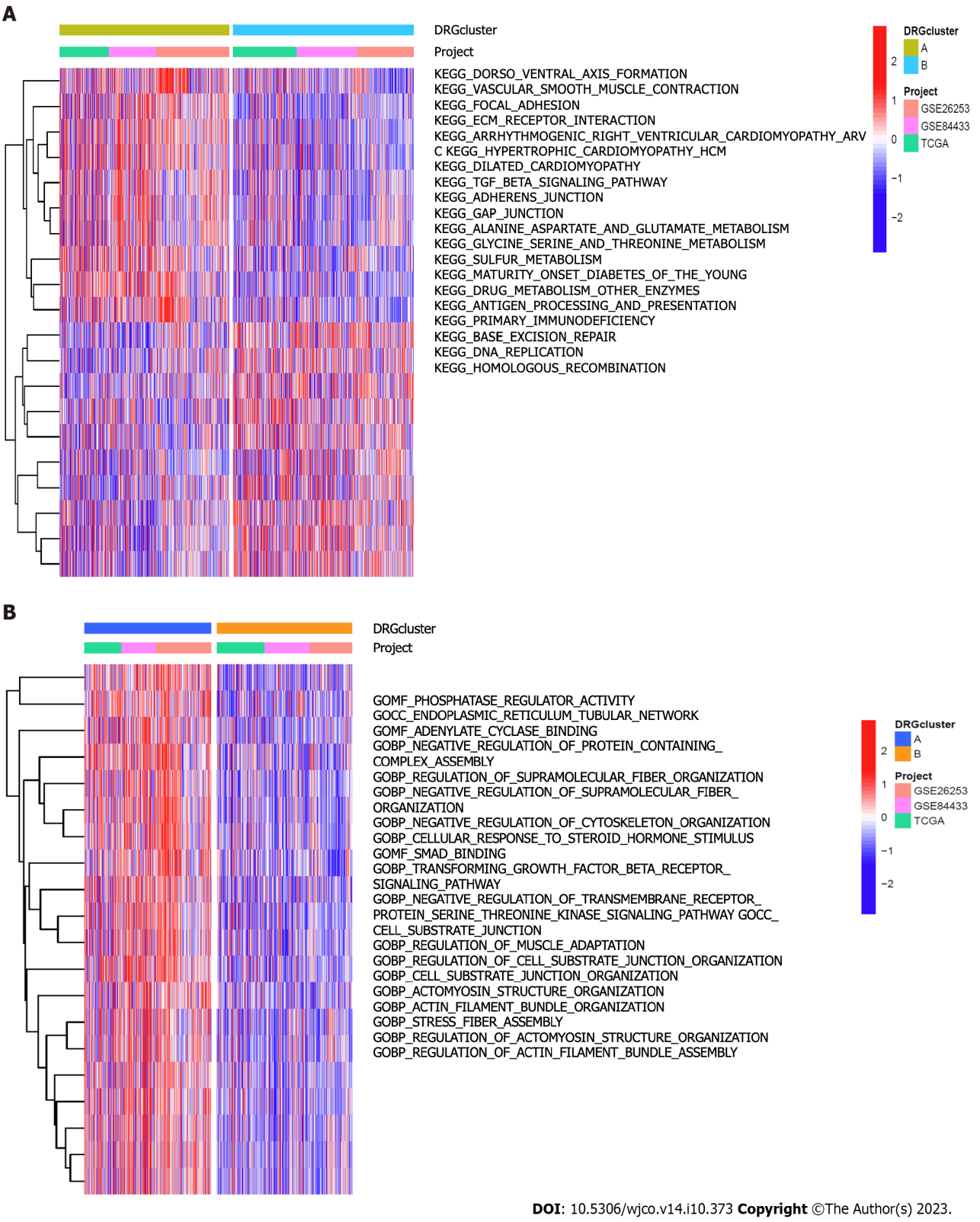

DOI: 10.5306/wjco.v14.i10.373

Figure 4 The significantly different kyoto encyclopedia of genes and genomes pathways and gene ontology functional analysis between disulfidptosis related genes subgroups are presented. A: Shows the significantly different kyoto encyclopedia of genes and genomes pathway enrichment analysis between disulfidptosis related genes subgroups; B: Shows the significantly different gene ontology pathway enrichment analysis between disulfidptosis related genes subgroups.

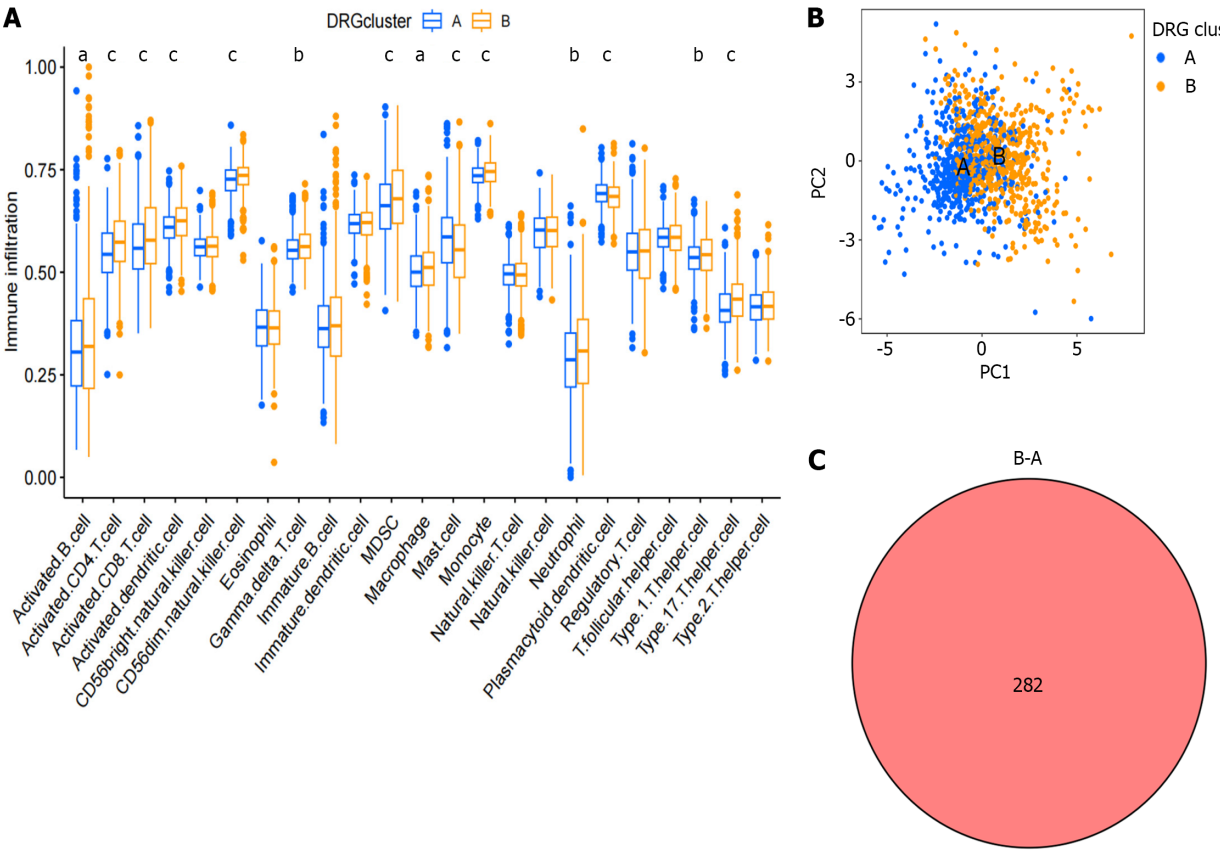
A
DRGcluster A B
Immune infiltration
1.00
0.75
0.50
0.25
0.00
a c c c c b c a c c b c b c
Activated.B.cell
Activated.CD4.T.cell
Activated.CD8.T.cell
Activated.dendritic.cell
CD56bright.natural.killer.cell
CD56dim.natural.killer.cell
Eosinophil
Gamma.delta.T.cell
Immature.B.cell
Immature.dendritic.cell
MDSC
Macrophage
Mast.cell
Monocyte
Natural.killer.T.cell
Natural.killer.cell
Neutrophil
Plasmacytoid.dendritic.cell
Regulatory.T.cell
T.follicular.helper.cell
Type.1.T.helper.cell
Type.17.T.helper.cell
Type.2.T.helper.cell
B
DRG cluster
A
B
PC2
PC1
3
0
-3
-6
-5
0
5
C
B-A
282

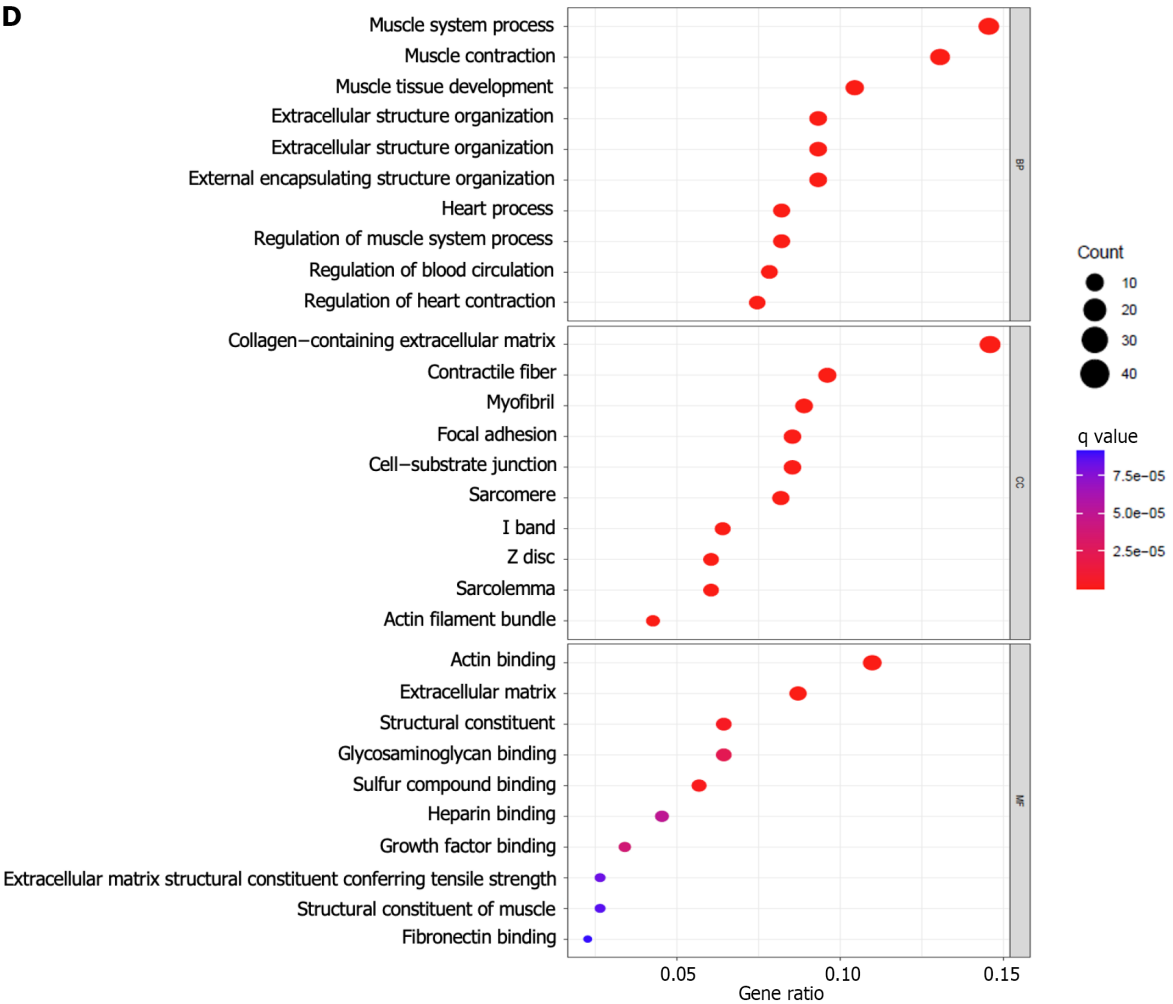
D
Muscle system process
Muscle contraction
Muscle tissue development
Extracellular structure organization
Extracellular structure organization
External encapsulating structure organization
Heart process
Regulation of muscle system process
Regulation of blood circulation
Regulation of heart contraction
Collagen−containing extracellular matrix
Contractile fiber
Myofibril
Focal adhesion
Cell−substrate junction
Sarcomere
I band
Z disc
Sarcolemma
Actin filament bundle
Actin binding
Extracellular matrix
Structural constituent
Glycosaminoglycan binding
Sulfur compound binding
Heparin binding
Growth factor binding
Extracellular matrix structural constituent conferring tensile strength
Structural constituent of muscle
Fibronectin binding
BP
CC
MF
0.05
0.10
0.15
Gene ratio
Count
10
20
30
40
q value
7.5e−05
5.0e−05
2.5e−05

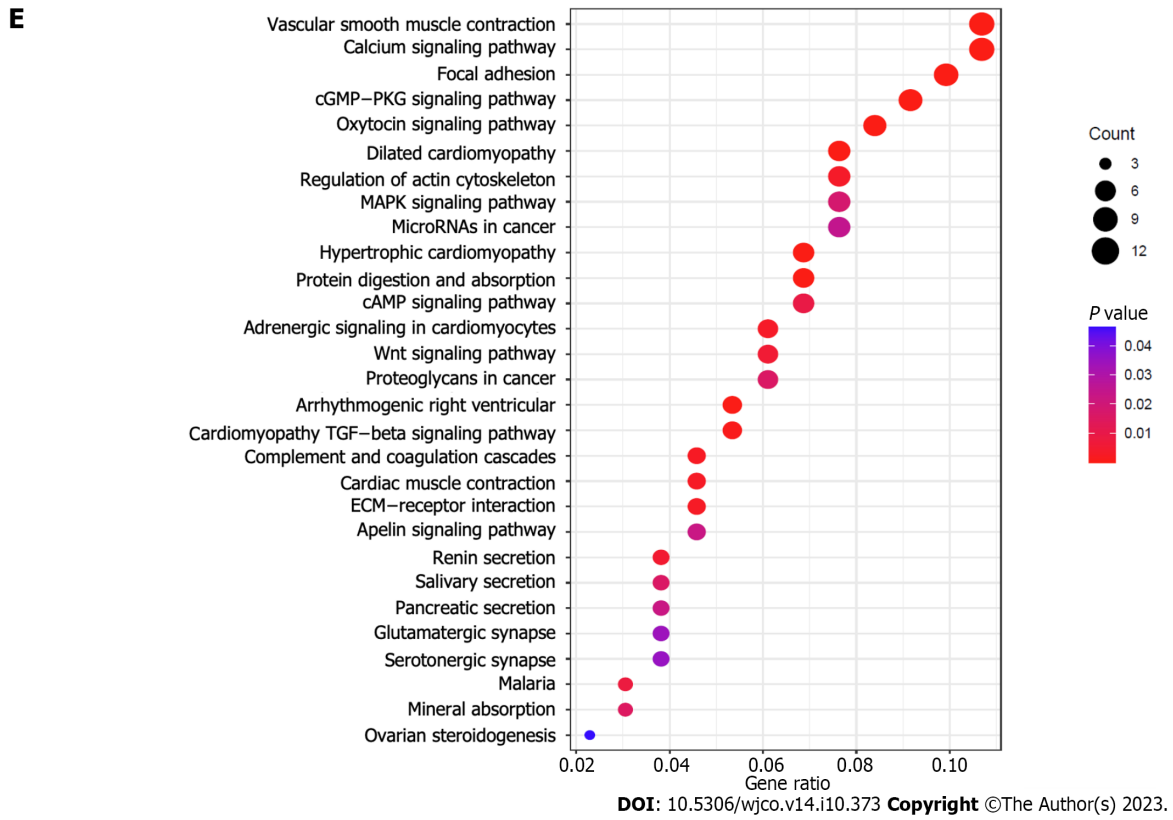

DOI: 10.5306/wjco.v14.i10.373

Figure 5 The immune cell differential analysis, principal component analysis analysis, significantly different genes, and gene ontology/kyoto encyclopedia of genes and genomes analysis between disulfidptosis related genes subgroups are presented. A: Shows the immune cell differential analysis between disulfidptosis related genes subgroups; B: Presents the principal component analysis analysis of disulfidptosis related genes subgroups; C: Shows the significantly different genes between disulfidptosis related genes subgroups; D: Presents the gene ontology analysis of significantly different genes between disulfidptosis related genes subgroups; E: Presents the kyoto encyclopedia of genes and genomes analysis of significantly different genes between disulfidptosis related genes subgroups.

high- and low-risk groups for the overall, test set, and training set samples. We then performed survival, ROC, and risk analyses on each group. Survival analysis of each group revealed that the high-risk group had poorer prognosis than the low-risk group (Figure 8A-C). Through ROC curve analysis of each group, we found that the area under the curve values of the overall, training set, and test set samples for 1, 3, and 5 years were all > 0.05, indicating the accuracy of the model in predicting survival prognosis (Figure 8D-F). Risk curve analysis of the total, training set, and test set samples showed an increase in the number of deaths with an increase in the risk score. We also found that *VAMP7* was a low-risk gene, while *PLS3*, *GRP*, *APOD*, *SGCE*, and *COL8A1* were high-risk genes through heatmap analysis (Figure 8G-O). Comparison of the results of survival, ROC, and risk analyses among various groups showed that the results were consistent, indicating the accuracy of this risk model in predicting the prognosis of patients with GC.

Identification of potential therapeutic targets by constructing column line graphs and immune and drug sensitivity analyses

We found that *APOD*, *PLS3*, age, sex, and N staging are independent factors that impact patient prognosis, all of which are risk factors for the prognosis of patients with GC. The odds of patients surviving for 1, 3, and 5 years are 0.806, 0.527, and 0.39, respectively (Figure 9A). The correction curve shows that the predicted value of the model is close to the actual value (Figure 9B). Through immune cell analysis, we found that resting mast cells and *APOD* were significantly positively correlated. Moreover, *PLS3* was significantly positively correlated with resting mast cells (Figure 9C). We also conducted survival analysis on *APOD* and *PLS3* by GEPIA, which were found to have independent effects on the prognosis of GC through column line graph analysis, and found that the survival analysis of *APOD* showed significant differences ($P < 0.05$) (Figure 9D), while the survival analysis of *PLS3* did not indicate the presence of significant differences ($P > 0.05$) (Figure 9E). In the relationship analysis between immune cells and risk scores, we found that 13 types of immune cells were significantly correlated with risk scores (Figure 10). Through TME scoring, we found differences between high and low risk groups in terms of the Stromal Score and ESTIMATE Score, both of which were upregulated in the high-risk group (Figure 11A). The waterfall chart shows that the genes that undergo mutations in the high- and low-risk groups were consistent, while the probability of mutations occurring in the low-risk group was higher than that in the high-risk group (Figure 11B and C). Through TMB analysis, we found significant differences between the high- and low-risk groups, as well as a negative correlation between TMB and risk scores (Figure 11D and E). Through microsatellite instability analysis, we found significant differences between the microsatellite stability and MSI-high (MSI-

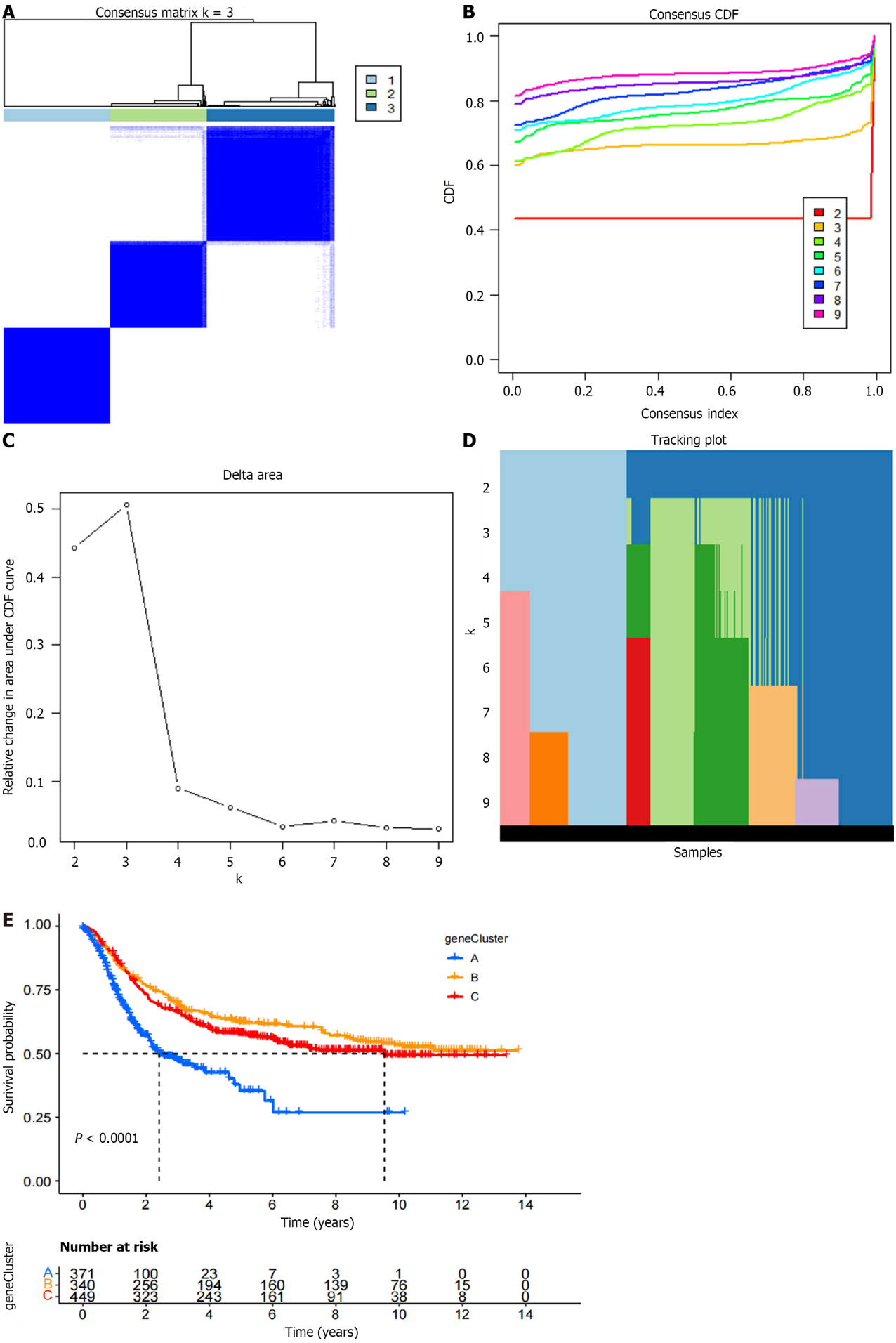
A
Consensus matrix k = 3
1
2
3
B
Consensus CDF
CDF
Consensus index
2
3
4
5
6
7
8
9
C
Delta area
Relative change in area under CDF curve
k
D
Tracking plot
k
Samples
E
geneCluster
A
B
C
Surivival probability
P < 0.0001
Time (years)
Number at risk
geneCluster
A 371 100 23 7 3 1 0 0
B 340 256 194 160 139 76 15 0
C 449 323 243 161 91 38 8 0
Time (years)

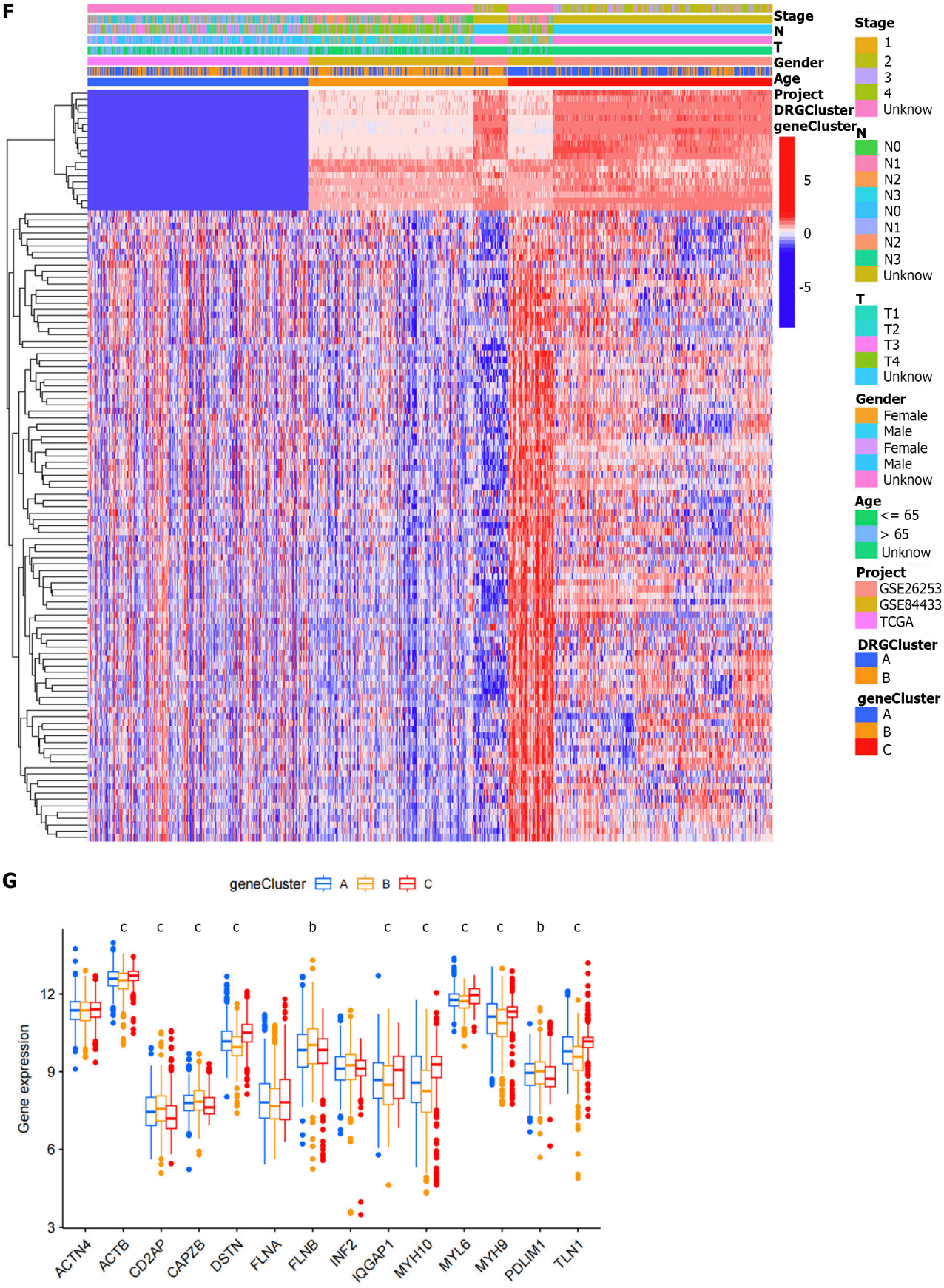
F
Stage
N
T
Gender
Age
Project
DRGCluster
geneCluster
5
0
-5
Stage
1
2
3
4
Unknow
N
N0
N1
N2
N3
N0
N1
N2
N3
Unknow
T
T1
T2
T3
T4
Unknow
Gender
Female
Male
Female
Male
Unknow
Age
<= 65
> 65
Unknow
Project
GSE26253
GSE84433
TCGA
DRGCluster
A
B
geneCluster
A
B
C
G
geneCluster A B C
c c c c b c c c c b c
Gene expression
12
9
6
3
ACTN4
ACTB
CD2AP
CAPZB
DSTN
FLNA
FLNB
INF2
IQGAP1
MYH10
MYL6
MYH9
PDLIM1
TLN1

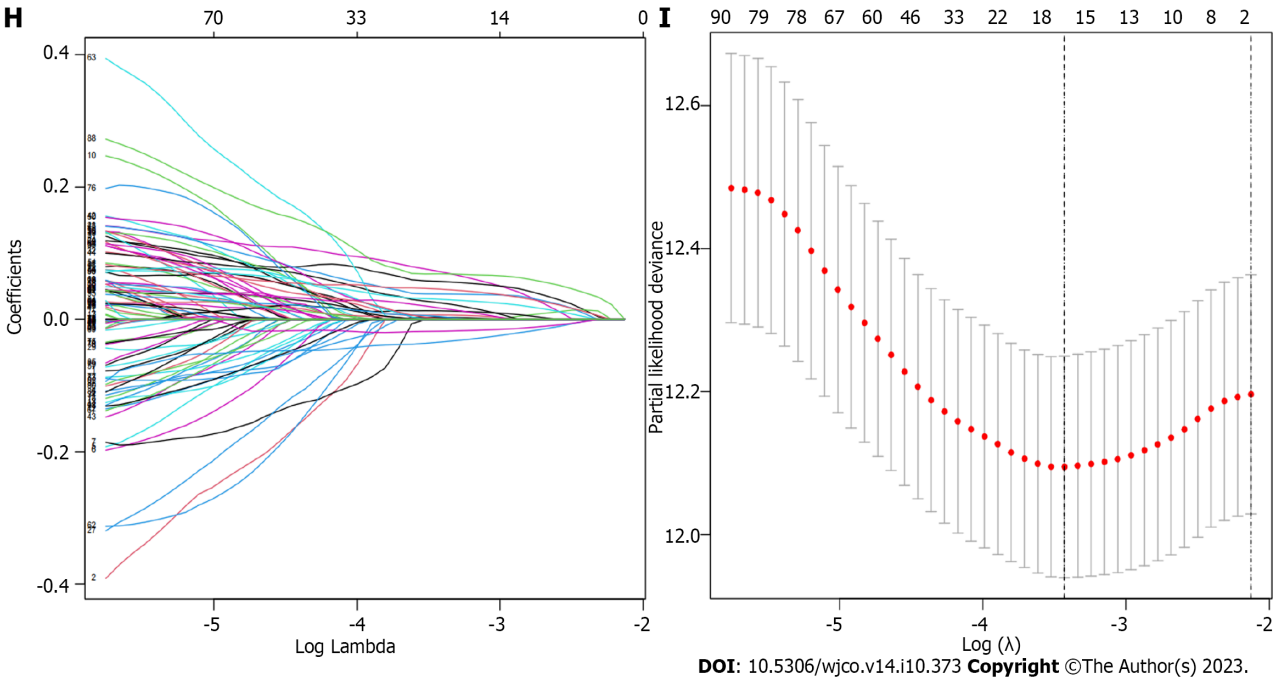

DOI: 10.5306/wjco.v14.i10.373

Figure 6 The differential gene-related sample clustering matrix, clustering index, cumulative distribution function curve, tracking plot, survival curve, heat map, differential analysis of disulfidptosis related genes, lasso regression plot, and cvfit plot are presented. A: Shows the clustering matrix of differential gene-related samples; B: Presents the clustering index of differential gene-related samples; C: Shows the relative change area of the cumulative distribution function curve of differential gene-related samples; D: Presents the tracking plot of differential gene subgroups; E: Shows the survival curve of differential gene-related samples; F: Presents the heat map of differential gene-related samples; G: Presents the differential analysis of disulfidptosis related genes between differential gene-related sample groups; H: Shows the lasso regression plot; I: Presents the cvfit plot of the lasso regression.

H) groups, as well as between the MSI-H and MSI-low groups. The risk value of the MSI-H group is the lowest, and the proportion of stable samples in the high-risk group is as high as 71% (Figure 11F and G). Stem cell correlation analysis shows that RNA stemness scores (RNAss) is negatively correlated with risk scores (Figure 11H). Finally, drug analysis showed significant differences in the sensitivity of 89 drugs, including Bosutinib and Bryostatin (Figure 11I and J), between high- and low-risk groups.

Immunohistochemical analysis

Through the HPA network database, immunohistochemical analysis of *APOD* revealed that the protein expression level of *APOD* in GC tissues was significantly higher than that in normal tissues adjacent to GC (Figure 12).

DISCUSSION

The occurrence and development of GC are complex pathological processes involving the activation and alteration of multiple genes and signaling pathways[66]. Previous studies have shown that the expression of certain genes in GC tissue and normal gastric tissue can vary[67]. In this study, we analyzed the differential expression of 10 DRGs between GC tissue and adjacent normal tissue and found significant differences between the two. By analyzing the mutation waterfall plot and mutation frequency plot of DRGs, we observed that most DRGs were mutated in GC tissue, further indicating that DRGs are differentially expressed in cancer tissue. Previous studies have found that high expression of the disulfidptosis-related gene *PDLIM1* may inhibit the proliferation, invasion, and migration of GC cells, promote apoptosis, and enhance their sensitivity to cisplatin[68]. It has also been found that the high expression of *FLNA* can lead to low survival rate and migration and invasion energy of GC cells[69]. Additionally, the disulfidptosis-related gene *MYH10* may be related to the occurrence, development, and drug resistance of ovarian cancer[70], but its role in GC requires further exploration. Moreover, previous studies have revealed that *DSTN* increases the colony formation and migration ability of tumor cells when highly expressed[71], although its relationship with GC prognosis requires further study. Study on *MYL6* revealed possible impacts on the migration of melanoma cells[72], but its relationship with GC needs further study. In this study, we found that *PDLIM1*, *FLNA*, *MYH10*, *MYL6*, and *DSTN* are significantly associated with GC prognosis ($P < 0.05$), among which, *DSTN*, *FLNA*, *MYH10*, and *MYL6* are risk factors for GC prognosis, while *PDLIM1* is a protective factor for GC prognosis. Our study further demonstrates the impact of DRGs on GC prognosis.

Our results revealed significant pathway and functional differences, as well as significantly different KEGG and GO pathways and functions between the two subtypes of disulfidptosis, mainly enriched in amino acid metabolism, TGF-β signaling pathway, pentose phosphate pathway, Wnt signaling pathway, and MAPK signaling pathway, among others. These functions and pathways may be related to the presence of GC. Indeed, previous studies have found that the TGF-β

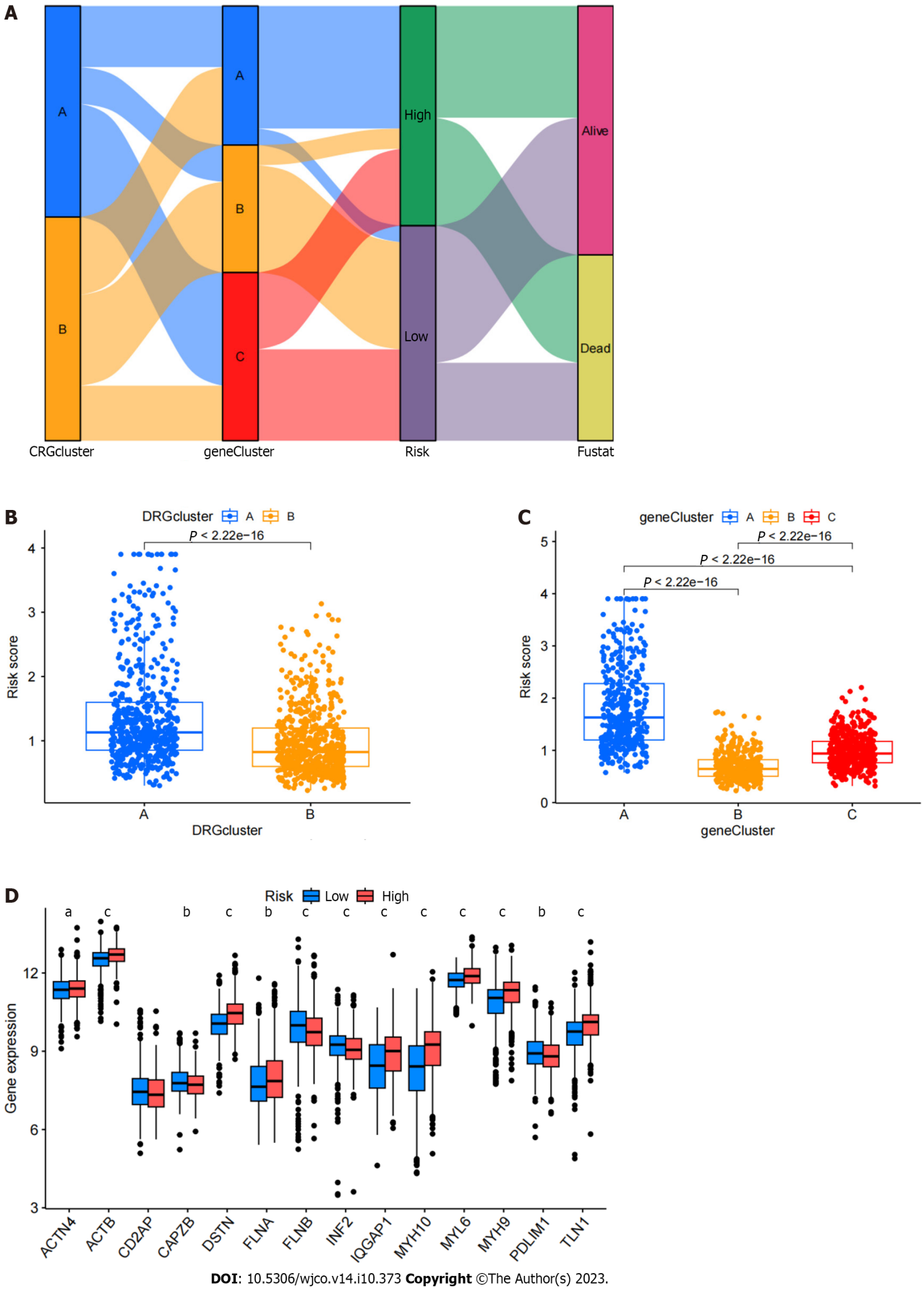

DOI: 10.5306/wjco.v14.i10.373

Figure 7 Testing the reliability of prognostic models. A: A Sankey diagram of the relationships between various data is presented; B: Shows a box plot of the disulfidptosis subtype; C: Presents a box plot of gene subtypes; D: Shows the differential analysis of disulfidptosis related genes between high and low-risk groups.

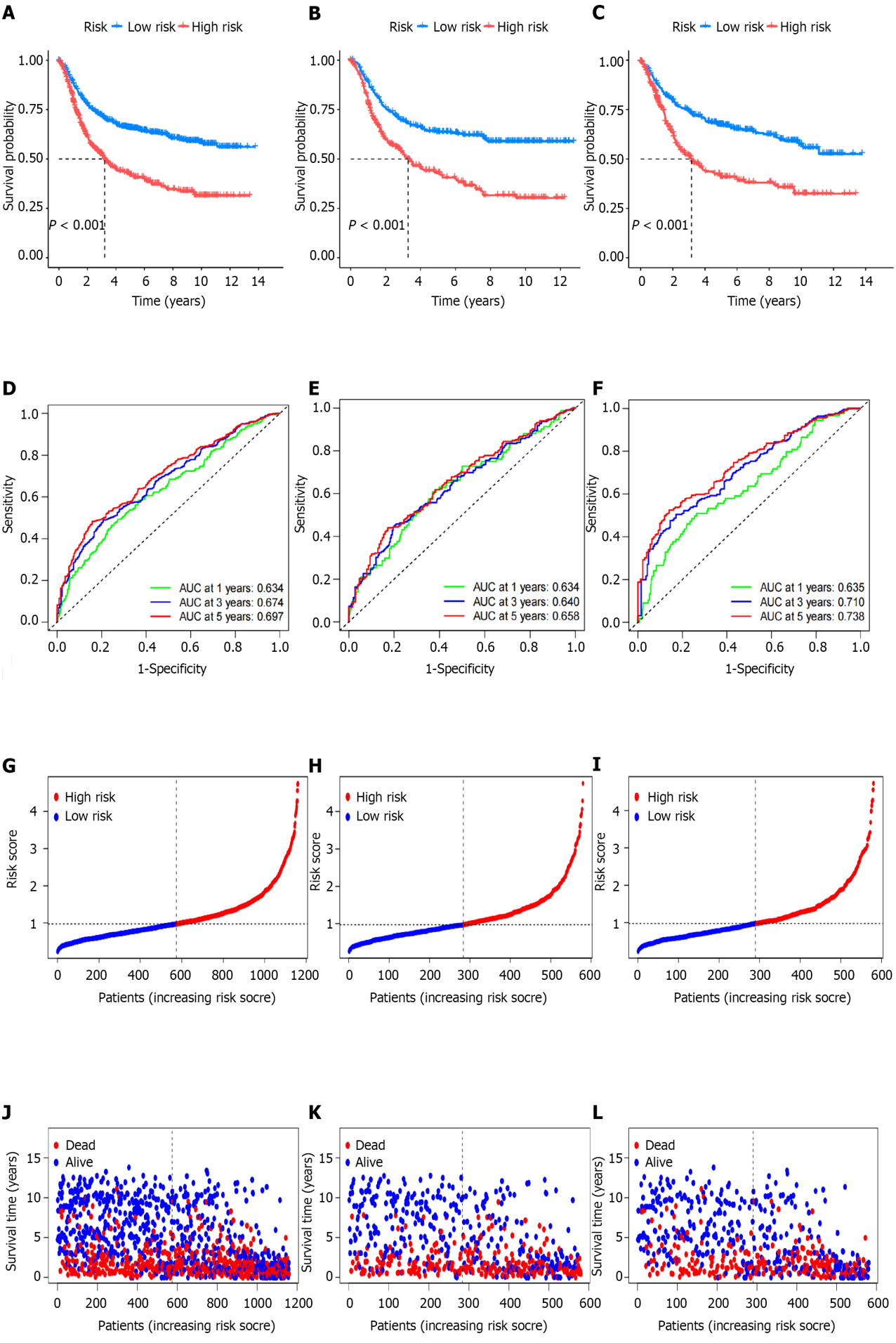
A
Risk Low risk High risk
Survival probability
P < 0.001
Time (years)
B
Risk Low risk High risk
Survival probability
P < 0.001
Time (years)
C
Risk Low risk High risk
Survival probability
P < 0.001
Time (years)
D
Sensitivity
AUC at 1 years: 0.634
AUC at 3 years: 0.674
AUC at 5 years: 0.697
1-Specificity
E
Sensitivity
AUC at 1 years: 0.634
AUC at 3 years: 0.640
AUC at 5 years: 0.658
1-Specificity
F
Sensitivity
AUC at 1 years: 0.635
AUC at 3 years: 0.710
AUC at 5 years: 0.738
1-Specificity
G
High risk
Low risk
Risk score
Patients (increasing risk socre)
H
High risk
Low risk
Risk score
Patients (increasing risk socre)
I
High risk
Low risk
Risk score
Patients (increasing risk socre)
J
Dead
Alive
Survival time (years)
Patients (increasing risk socre)
K
Dead
Alive
Survival time (years)
Patients (increasing risk socre)
L
Dead
Alive
Survival time (years)
Patients (increasing risk socre)

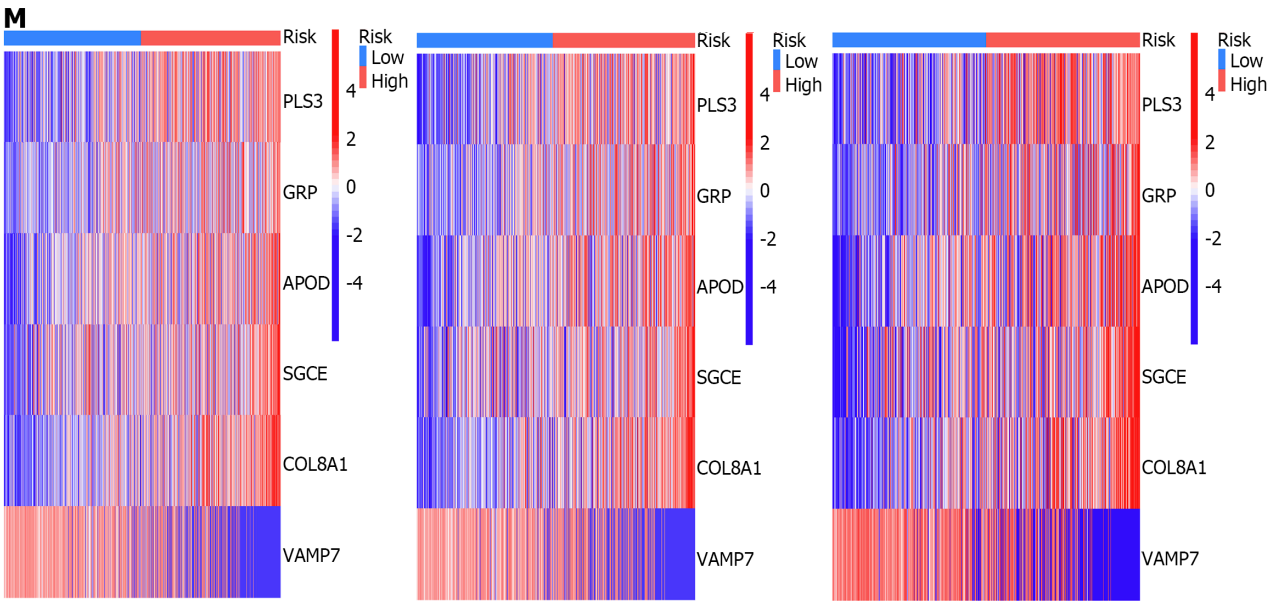

DOI: 10.5306/wjco.v14.i10.373

Figure 8 The accuracy of the prognostic model was verified by subgroup analysis. A-C: Survival curves between different groups are presented in panels; D-F: Show receiver operating characteristic curves between different groups; G-I: Risk curves for each group are presented; J-L: Show survival status plots for each group; M-O: Risk heat maps for each group are presented.

signaling pathway may be involved in the occurrence, invasion, proliferation, and metastasis of GC, affecting the prognosis of patients with GC[73-77]. Furthermore, some studies have suggested that the pentose phosphate pathway may be related to the proliferation of GC cells[78]. Previous studies have also found that the MAPK signaling pathway may also be involved in the occurrence, invasion, proliferation, and metastasis of GC, affecting the prognosis of GC[79-87]. Additionally, some studies have found that the Wnt signaling pathway may be involved in the metastasis, migration, invasion, and progression of GC, affecting the prognosis of GC[88-94]. In the current study, we also found differences in immune cell infiltration between the subgroups of disulfidptosis gene typing. Taken together, these findings and research suggest that DRGs affect various aspects of patients with GC, including amino acid metabolism, various signaling pathways, and immune cell infiltration, all of which may affect the survival or prognosis of patients with GC; however, the specific mechanisms and functions need to be further explored.

In this study, we used a risk model to score differentially expressed genes in overall, training set, and testing set samples, dividing them into high- and low-risk groups. Survival, ROC, and risk analyses were conducted for each group. The results showed that the high-risk group had a poorer prognosis than the low-risk group in all groups, and the result trend was consistent, further demonstrating the reliability of the model.

Through column line chart analysis, we revealed that *APOD*, *PLS3*, age, sex, and N stage represent independent risk factors affecting patient prognosis, all of which are risk factors for GC prognosis. Through column line chart analysis, we observed that the survival rates of patients at 1, 3, and 5 years gradually decreased, with rates of 0.806, 0.527, and 0.39, respectively; this is consistent with the trend of 1-, 3-, and 5-year survival rates in previous studies on GC, further confirming the reliability of the prognostic model[95]. Additionally, we found that *APOD* represents an independent prognostic factor for GC in this model ($P < 0.001$). Previous studies on *APOD* have found that it may be involved in the construction of multiple GC prognostic and immune prediction models[96-103], which may be related to GC prognosis. In this study, we further analyzed the protein encoded by *APOD* in the HPA network database through immunohistochemical analysis and found that its protein expression level in GC tissues was significantly higher than that in adjacent normal tissues, further indicating significant differences in *APOD* between GC tissues and adjacent normal tissues. Overall, our results suggest that *APOD* may play an important role in the occurrence and development of GC, while its expression level may be related to the prognosis of patients with GC, further suggesting that *APOD* represents a potential therapeutic target for GC.

We also found that the genes constituting the GC prognosis model were related to various immune cells, indicating that the DRGs may affect the immunity of patients with GC. The heatmap of the correlation between the model genes and immune cells in this study showed a significant positive correlation between disulfidptosis *PLS3* and resting mast cells ($P < 0.001$). Indeed, previous studies have found a correlation between resting mast cells and GC[104,105], and it has been suggested that *PLS3*[106] may also be related to GC. Through the analysis of TME differences in the prognosis model, we found differences in the Stromal Score and ESTIMATE Score in the high- and low-risk groups, with both scores found to be upregulated in the high-risk group, indicating that the risk score of the prognosis model is related to the TME of GC. Through the analysis of the relationship between the risk score of the prognosis model and TMB, MSI, and stem cell correlation, we found that the risk score of the prognosis model was correlated with TMB, MSI, and RNAss. These results further indicate that the DRGs may be related to the immunity or immune therapy targets of TMB, MSI, and RNAss in patients with GC, which may affect the immune therapy effect and prognosis of patients with GC. Among them, MSI, an

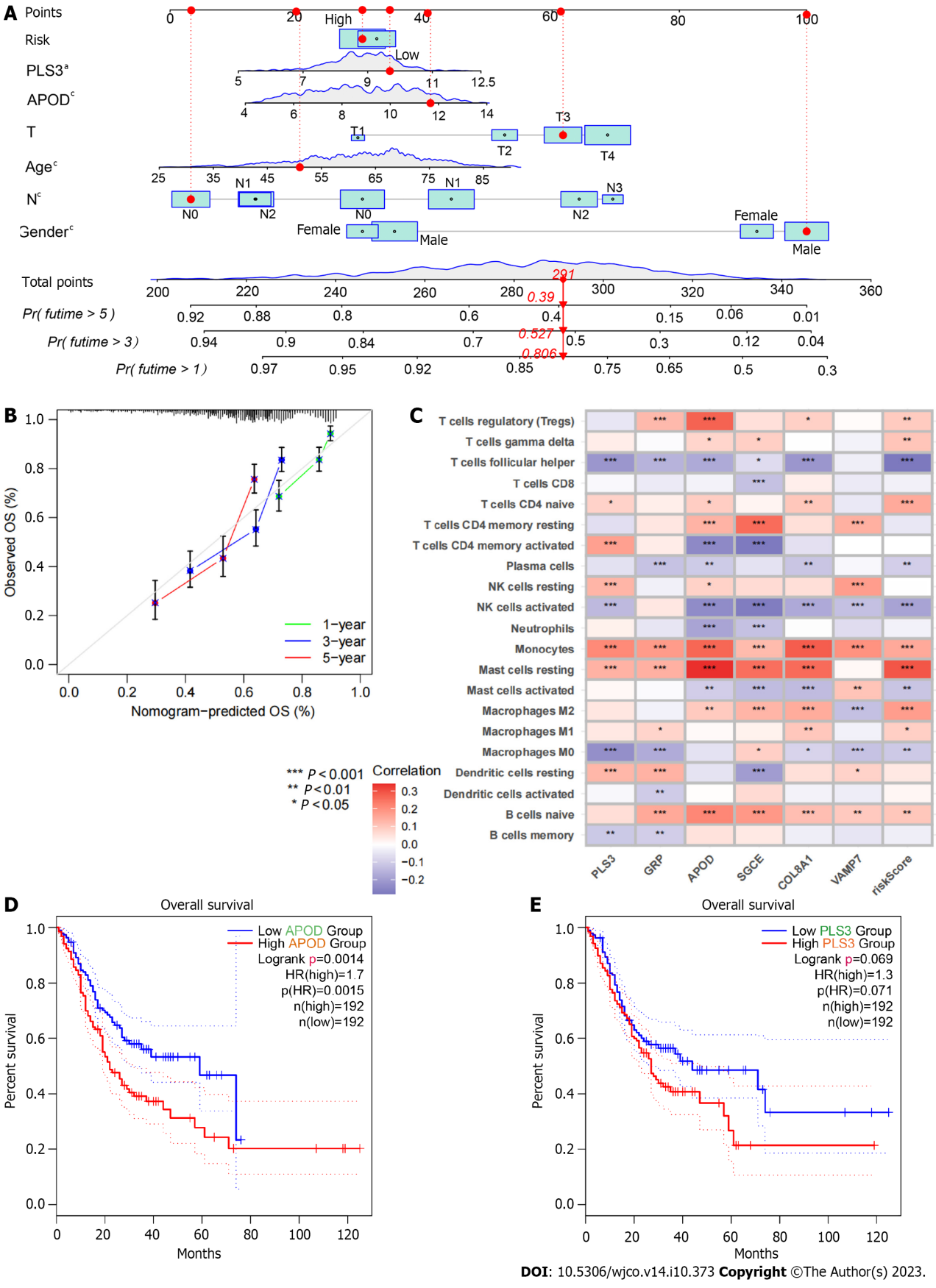

DOI: 10.5306/wjco.v14.i10.373

Figure 9 Further analysis of prognostic models to screen potential therapeutic targets. A: Presents a column line chart; B: Shows a calibration curve; C: Presents a heat map of the correlation between model genes and immune cells; D:The survival curve of *APOD* in gastric cancer was significantly different between high and low risk groups ($P < 0.05$); E: The survival curve of *PLS3* in gastric cancer was shown between high and low risk groups, and the results suggested that the difference was not significant ($P > 0.05$).

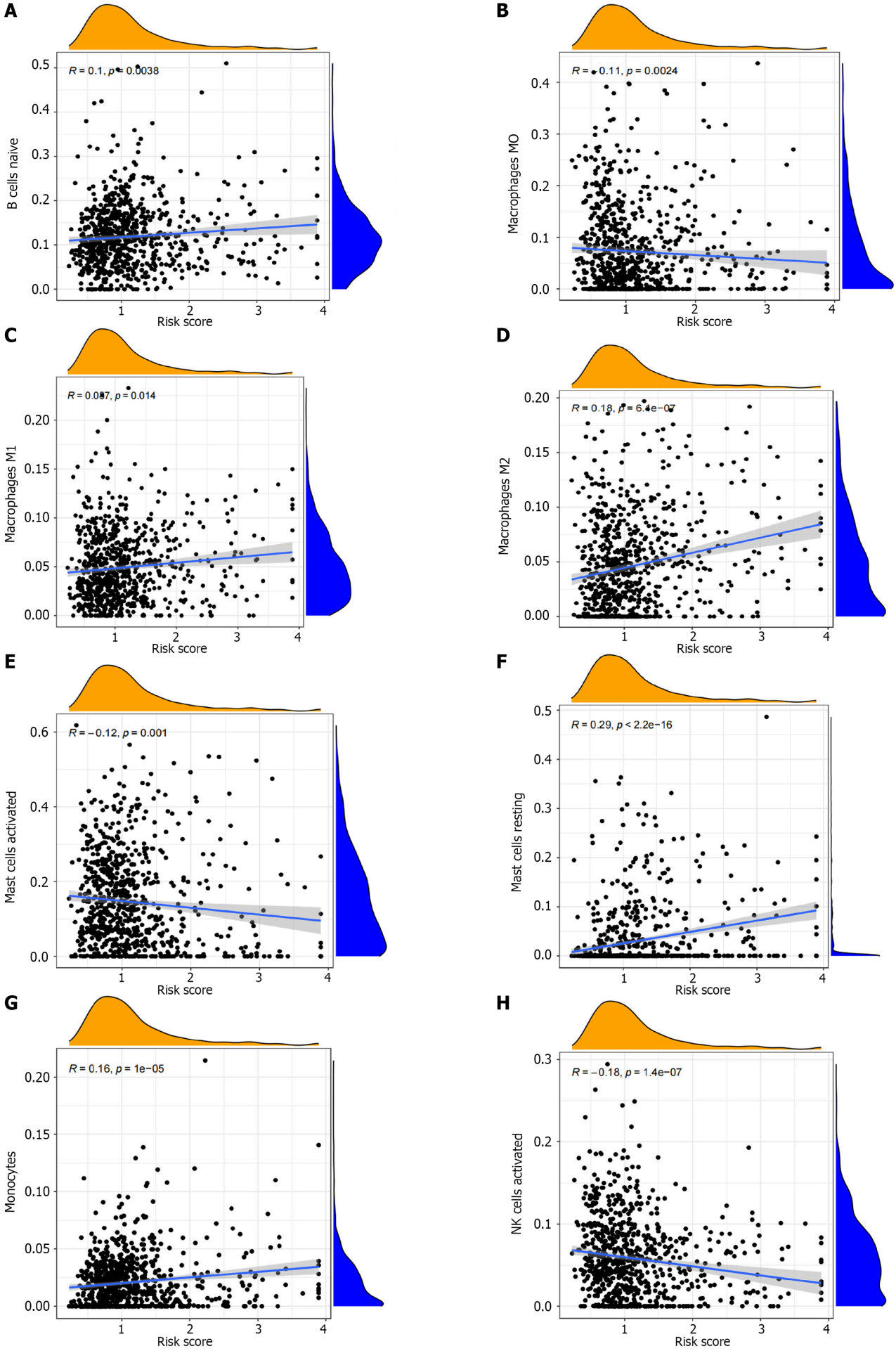
A
R = 0.1, p = 0.0038
B cells naive
Risk score
B
R = 0.11, p = 0.0024
Macrophages M0
Risk score
C
R = 0.087, p = 0.014
Macrophages M1
Risk score
D
R = 0.18, p = 6.4e−07
Macrophages M2
Risk score
E
R = −0.12, p = 0.001
Mast cells activated
Risk score
F
R = 0.29, p < 2.2e−16
Mast cells resting
Risk score
G
R = 0.16, p = 1e−05
Monocytes
Risk score
H
R = −0.18, p = 1.4e−07
NK cells activated
Risk score

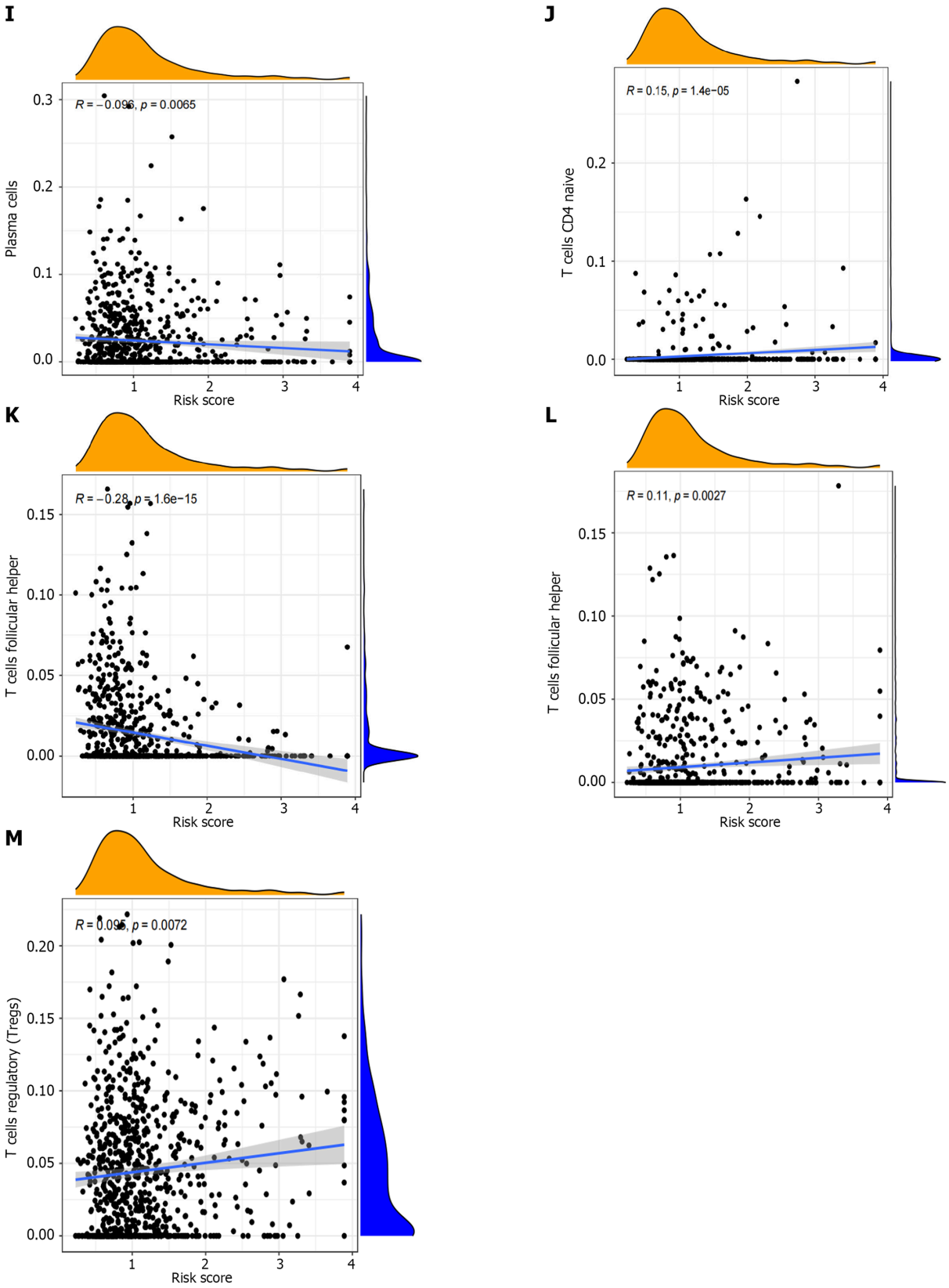

DOI: 10.5306/wjco.v14.i10.373

Figure 10 The correlation between immune cells and risk scores is analyzed. A: There was a positive correlation between B cells naive and risk score; B: The result shows that macrophages M0 is negatively correlated with risk score; C: The results showed that macrophages M1 was positively correlated with risk score; D: The results showed that macrophages M2 was positively correlated with risk score; E: There was a negative correlation between mast cells activated and risk score; F: The results showed that mast cells reting was positively correlated with risk score; G: There was a positive correlation between monocytes and risk score; H: There was a negative correlation between natural killer cells activated and risk score; I: There was a negative correlation between plasma cells and risk score; J: There was a positive correlation between T cells CD4 naive and risk score; K: It showed that T cells follicular helper was negatively correlated with risk score; L: There was a positive correlation between T cells gamma delta and risk score; M: There was a positive correlation between T cells regulation and risk score.

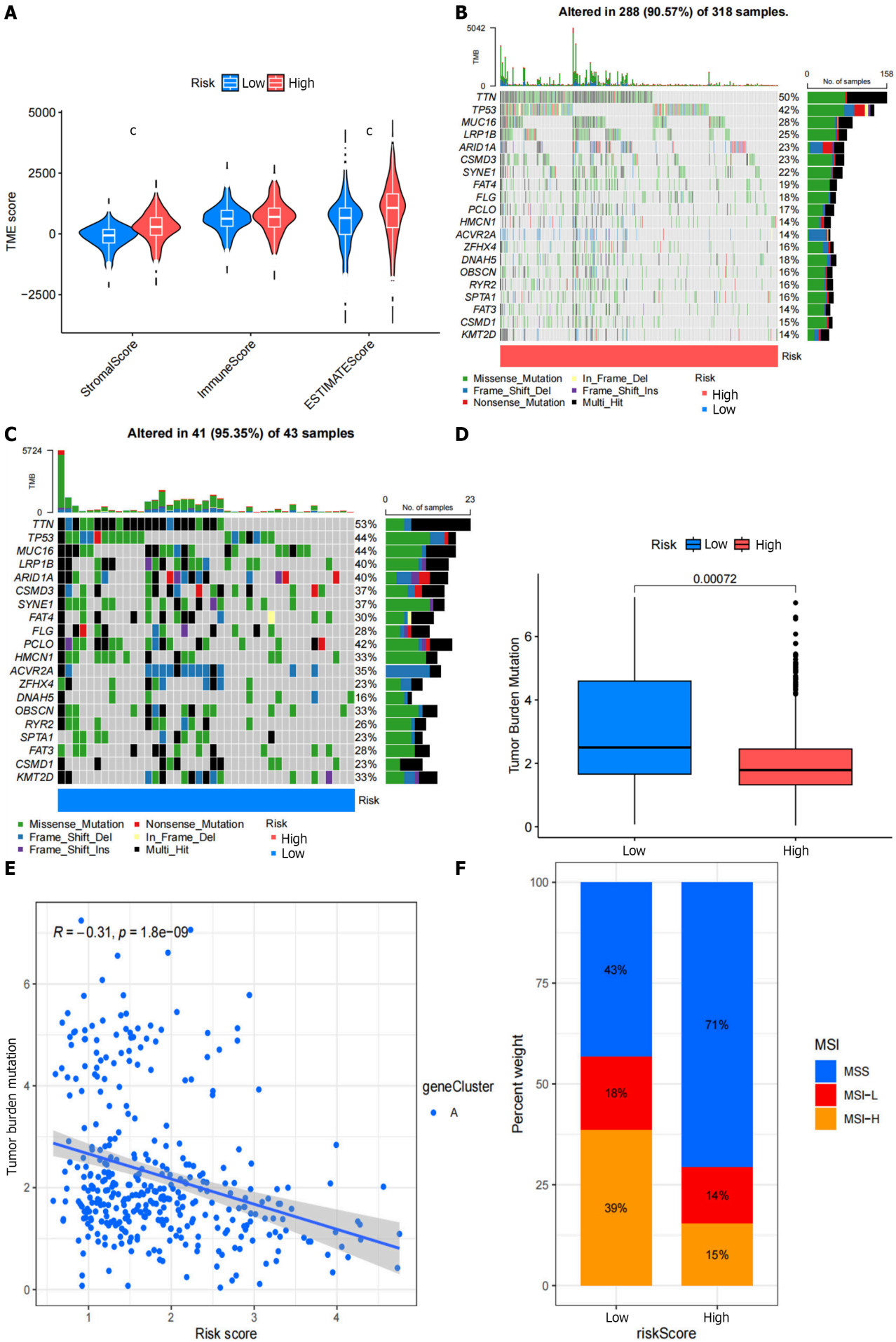
A
Risk Low High
TME score
5000
2500
0
−2500
c
c
StromalScore
ImmuneScore
ESTIMATEScore
B
Altered in 288 (90.57%) of 318 samples.
TMB
5042
0
No. of samples
0
158
TTN 50%
TP53 42%
MUC16 28%
LRP1B 25%
ARID1A 23%
CSMD3 23%
SYNE1 22%
FAT4 19%
FLG 18%
PCLO 17%
HMCN1 14%
ACVR2A 14%
ZFHX4 16%
DNAH5 18%
OBSCN 16%
RYR2 16%
SPTA1 16%
FAT3 14%
CSMD1 15%
KMT2D 14%
Risk
Missense_Mutation
Frame_Shift_Del
Nonsense_Mutation
In_Frame_Del
Frame_Shift_Ins
Multi_Hit
Risk
High
Low
C
Altered in 41 (95.35%) of 43 samples
TMB
5724
0
No. of samples
0
23
TTN 53%
TP53 44%
MUC16 44%
LRP1B 40%
ARID1A 40%
CSMD3 37%
SYNE1 37%
FAT4 30%
FLG 28%
PCLO 42%
HMCN1 33%
ACVR2A 35%
ZFHX4 23%
DNAH5 16%
OBSCN 33%
RYR2 26%
SPTA1 23%
FAT3 28%
CSMD1 23%
KMT2D 33%
Risk
Missense_Mutation
Frame_Shift_Del
Frame_Shift_Ins
Nonsense_Mutation
In_Frame_Del
Multi_Hit
Risk
High
Low
D
Risk Low High
0.00072
Tumor Burden Mutation
0
2
4
6
Low
High
E
R = −0.31, p = 1.8e−09
Tumor burden mutation
0
2
4
6
1
2
3
4
Risk score
geneCluster
A
F
Percent weight
0
25
50
75
100
43%
18%
39%
71%
14%
15%
Low
High
riskScore
MSI
MSS
MSI-L
MSI-H

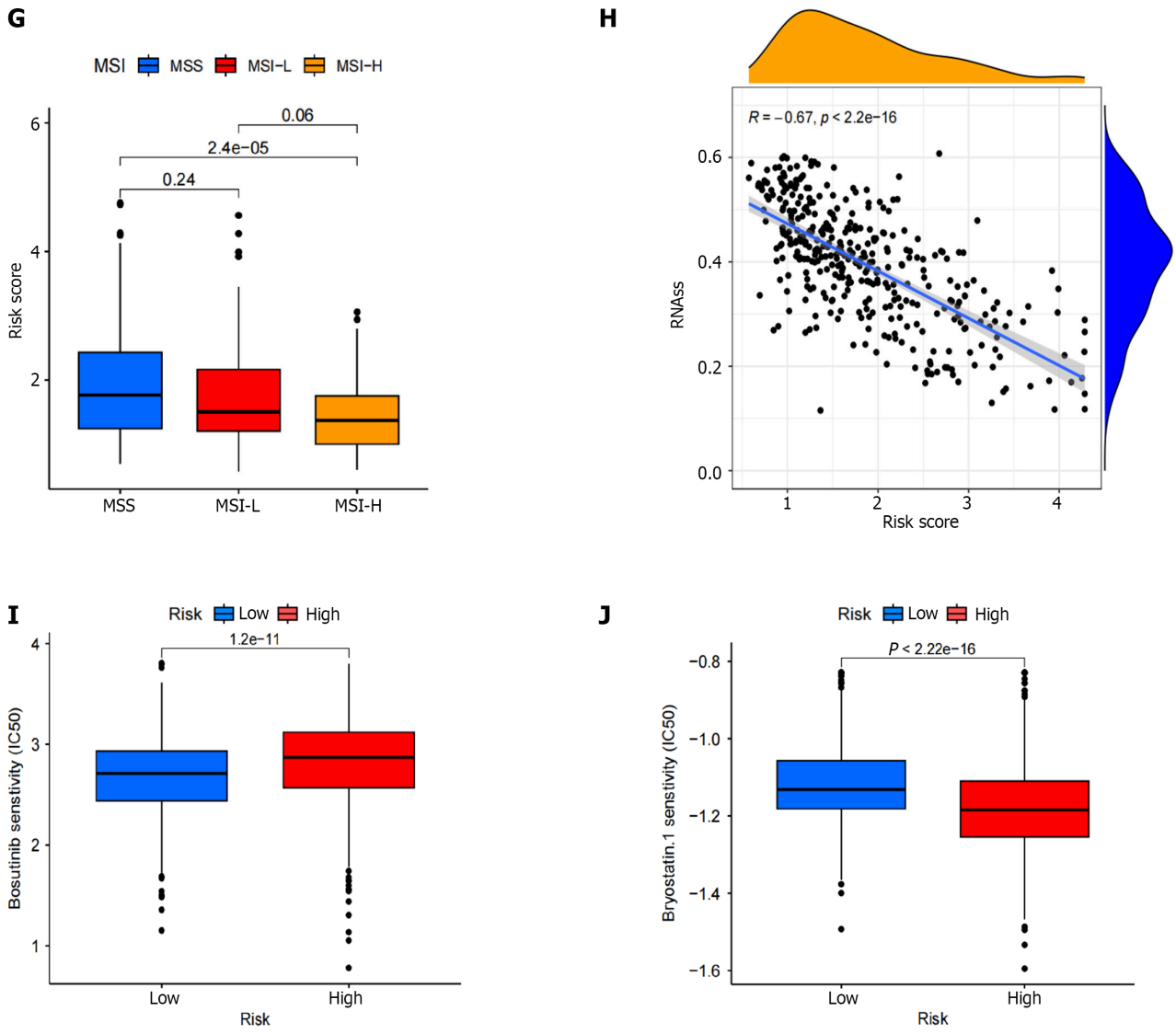

DOI: 10.5306/wjco.v14.i10.373 **Copyright** ©The Author(s) 2023.

Figure 11 The correlation between the prognostic scoring model and tumor microenvironment, microsatellite instability, and RNAss, as well as drug sensitivity analysis, is presented. A: Shows the tumor microenvironment score for high and low-risk groups; B and C: Present waterfall plots of mutations for high and low-risk groups; D: Analyzes the differences in tumor mutation burden between high and low-risk groups; E: Shows the relationship between tumor mutation burden and risk score; F and G: Present microsatellite instability analysis for high and low-risk groups; H: Analyzes the correlation between stem cells and risk score; I and J: Present drug sensitivity analysis for drugs such as Bosutinib and Bryostatin.

immune therapy target, has been found to affect the treatment and prognosis of patients with GC in previous studies[107-111], while the significant correlation between the GC risk prediction model established in this study and MSI indicates that MSI-targeted treatment may be meaningful for the treatment and prognosis of patients with GC. This further indicates the correlation between disulfidptosis and the immunity or immune therapy targets of patients with GC.

The results of our drug sensitivity analysis revealed that 89 drugs, including Bosutinib and Bryostatin, were significantly correlated with the sensitivity of GC treatment. Previous studies have found that Bryostatin can enhance the effect of paclitaxel in the treatment of GC[112], while others have found that Bosutinib may inhibit the migration of GC cells[113]. These results suggest that Bosutinib may have therapeutic effects on GC. The high sensitivity of Bosutinib and Bryostatin to GC found in this study suggests that they may be useful drugs for the treatment of GC. Therefore, the 89 drugs represented by Bosutinib in this study may be potential drugs for the treatment of GC.

CONCLUSION

In conclusion, our findings suggest that the DRGs and their submolecules may have an impact on immunity, immunotherapy targets, signaling pathways, and drug sensitivity in patients with GC. DRGs, including *PDLIM1*, *FLNA*, *MYH10*, *MYL6*, and *DSTN*, may be related to the prognosis of GC. Six genes, namely, *PLS3*, *GRP*, *APOD*, *SGCE*, *COL8A1*, and *VAMP7*, constituted a prognostic model of GC associated with DRG. *APOD* may be a potential target for the treatment of

GC, while 89 drugs, including Bosutinib and Bryostatin, may be potential drugs for the treatment of GC.

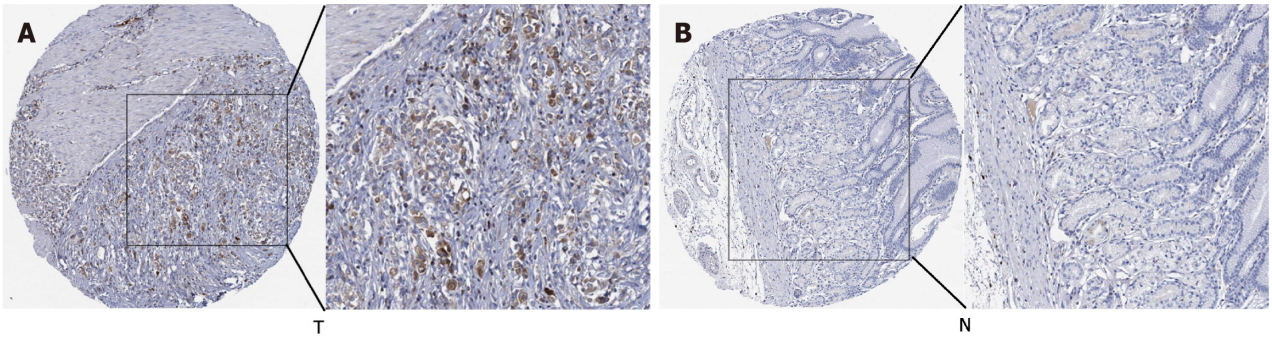

DOI: 10.5306/wjco.v14.i10.373 **Copyright** ©The Author(s) 2023.

Figure 12 The immunohistochemical analysis of the *APOD* gene based on human protein atlas is presented. A: Tumor tissue; B: Normal tissue. T: Tumor tissue; B: Normal tissue.

ARTICLE HIGHLIGHTS

Research background

Gastric cancer (GC) is one of the most common malignant tumors, although its pathogenesis remains unclear.

Research motivation

For the first time, in the current study, we constructed a new GC prognostic model based on the sub-group analysis of disulfidptosis-related genes (DRGs) and explored treatment targets and sensitive drugs.

Research objectives

The aims of this study were to explore a new GC prognostic model based on the sub-group analysis of DRGs and explore treatment targets and sensitive drugs.

Research methods

In this study, a bioinformatics strategy was used to extract GC-related data from The Cancer Genome Atlas and Gene Expression Omnibus databases, while R software (version 4.2.1) was used for correlation analysis.

Research results

Through the above analysis, we found that the didisulfidptosis-related gene may be related to the prognosis of GC. Six genes, namely, *PLS3*, *GRP*, *APOD*, *SGCE*, *COL8A1*, and *VAMP7*, constitute a predictive model for GC prognosis. *APOD* is a potential therapeutic target. Bosutinib and other drugs are suitable for the treatment of GC.

Research conclusions

The results of this study indicate that didisulfidptosis is related to the prognosis and treatment of GC. Additionally, *APOD* can be used as a potential therapeutic target for GC.

Research perspectives

Six genes, namely, *PLS3*, *GRP*, *APOD*, *SGCE*, *COL8A1*, and *VAMP7*, constitute a predictive model for GC prognosis. *APOD* is a potential therapeutic target for treating GC. Bosutinib and other drugs are suitable for the treatment of GC, although this requires further confirmation through molecular biology and clinical experiments.

FOOTNOTES

Author contributions: Li Q contributed to this work; Yin LK and Li Q prepared for the figures and tables; and all authors have approved the final manuscript.

Institutional review board statement: The data supporting the results of this study are available from Gene Expression Omnibus database (GSE84433andGSE26253) and the expression data, clinical data, mutation data, and copy data related to gastric cancer from The Cancer Genome Atlas database.

Conflict-of-interest statement: The authors deny any conflict of interest.

Data sharing statement: No additional data are available.

Country/Territory of origin: China

ORCID number: Qian Li 0009-0006-9250-0521; Long-Kuan Yin 0000-0001-5974-5443.

S-Editor: Qu XL
L-Editor: A
P-Editor: Zhang XD

REFERENCES

1 **Li Y**, Hu X, Lin R, Zhou G, Zhao L, Zhao D, Zhang Y, Li W, Ma P, Ren H, Liao X, Niu P, Wang T, Zhang X, Wang W, Gao R, Li Q, Church G, He J, Chen Y. Single-cell landscape reveals active cell subtypes and their interaction in the tumor microenvironment of gastric cancer. *Theranostics* 2022; **12**: 3818-3833 [PMID: 35664061 DOI: 10.7150/thno.71833]
2 **Chang X**, Ge X, Zhang Y, Xue X. The current management and biomarkers of immunotherapy in advanced gastric cancer. *Medicine (Baltimore)* 2022; **101**: e29304 [PMID: 35623069 DOI: 10.1097/MD.0000000000029304]
3 **Zhang Y**, Yu J. The role of MRI in the diagnosis and treatment of gastric cancer. *Diagn Interv Radiol* 2020; **26**: 176-182 [PMID: 32209504 DOI: 10.5152/dir.2019.19375]
4 **Smyth EC**, Nilsson M, Grabsch HI, van Grieken NC, Lordick F. Gastric cancer. *Lancet* 2020; **396**: 635-648 [PMID: 32861308 DOI: 10.1016/S0140-6736(20)31288-5]
5 **Machlowska J**, Baj J, Sitarz M, Maciejewski R, Sitarz R. Gastric Cancer: Epidemiology, Risk Factors, Classification, Genomic Characteristics and Treatment Strategies. *Int J Mol Sci* 2020; **21** [PMID: 32512697 DOI: 10.3390/ijms21114012]
6 **Zhao Q**, Cao L, Guan L, Bie L, Wang S, Xie B, Chen X, Shen X, Cao F. Immunotherapy for gastric cancer: dilemmas and prospect. *Brief Funct Genomics* 2019; **18**: 107-112 [PMID: 30388190 DOI: 10.1093/bfgp/ely019]
7 **Wu SL**, Zhang Y, Fu Y, Li J, Wang JS. Gastric cancer incidence, mortality and burden in adolescents and young adults: a time-trend analysis and comparison among China, South Korea, Japan and the USA. *BMJ Open* 2022; **12**: e061038 [PMID: 35863834 DOI: 10.1136/bmjopen-2022-061038]
8 **Yang X**, Zhang T, Zhang H, Sang S, Chen H, Zuo X. Temporal trend of gastric cancer burden along with its risk factors in China from 1990 to 2019, and projections until 2030: comparison with Japan, South Korea, and Mongolia. *Biomark Res* 2021; **9**: 84 [PMID: 34784961 DOI: 10.1186/s40364-021-00340-6]
9 **Gao M**, Yin H, Fei ZW. Clinical application of microRNA in gastric cancer in Eastern Asian area. *World J Gastroenterol* 2013; **19**: 2019-2027 [PMID: 23599620 DOI: 10.3748/wjg.v19.i13.2019]
10 **Tang D**, Liu S, Shen H, Deng G, Zeng S. Extracellular Vesicles Promote the Formation of Pre-Metastasis Niche in Gastric Cancer. *Front Immunol* 2022; **13**: 813015 [PMID: 35173726 DOI: 10.3389/fimmu.2022.813015]
11 **Gu X**, Zhang Y, Huang Y, Ju S. Comprehensive Evaluation of Serum tRF-17-WS7K092 as a Promising Biomarker for the Diagnosis of Gastric Cancer. *J Oncol* 2022; **2022**: 8438726 [PMID: 36245992 DOI: 10.1155/2022/8438726]
12 **Titov SE**, Anishchenko VV, Poloz TL, Veryaskina YA, Arkhipova AA, Ustinov SN. [Differential diagnostics of gastric cancer and precancerous changes of the gastric mucosa using analysis of expression of six microRNAS.]. *Klin Lab Diagn* 2020; **65**: 131-136 [PMID: 32159312 DOI: 10.18821/0869-2084-2020-65-2-131-136]
13 **Tong H**, Wang Y, Li Y, Liu S, Chi C, Liu D, Guo L, Li E, Wang C. Volatile organic metabolites identify patients with gastric carcinoma, gastric ulcer, or gastritis and control patients. *Cancer Cell Int* 2017; **17**: 108 [PMID: 29200968 DOI: 10.1186/s12935-017-0475-x]
14 **Zhao Y**, Zhou T, Li A, Yao H, He F, Wang L, Si J. A potential role of collagens expression in distinguishing between premalignant and malignant lesions in stomach. *Anat Rec (Hoboken)* 2009; **292**: 692-700 [PMID: 19306436 DOI: 10.1002/ar.20874]
15 **Qi M**, Liu D, Wang H, Bianba C, Ji W. Correlation of Single Nucleotide Gene Polymorphisms and Gastric Cancer Based on Magnetic Nanoparticles. *J Nanosci Nanotechnol* 2021; **21**: 928-934 [PMID: 33183426 DOI: 10.1166/jnn.2021.18628]
16 **Jiang L**, Gong X, Liao W, Lv N, Yan R. Molecular targeted treatment and drug delivery system for gastric cancer. *J Cancer Res Clin Oncol* 2021; **147**: 973-986 [PMID: 33550445 DOI: 10.1007/s00432-021-03520-x]
17 **Jiang H**, Hu K, Xia Y, Liang L, Zhu X. Long Noncoding RNA KLF3-AS1 Acts as an Endogenous RNA of miR-223 to Attenuate Gastric Cancer Progression and Chemoresistance. *Front Oncol* 2021; **11**: 704339 [PMID: 34745937 DOI: 10.3389/fonc.2021.704339]
18 **Guo XM**, Zhao HY, Shi ZY, Wang Y, Jin ML. [Application and Progress of Convolutional Neural Network-based Pathological Diagnosis of Gastric Cancer]. *Sichuan Da Xue Xue Bao Yi Xue Ban* 2021; **52**: 166-169 [PMID: 33829686 DOI: 10.12182/20210360501]
19 **Chen R**, Yang M, Huang W, Wang B. Cascades between miRNAs, lncRNAs and the NF-κB signaling pathway in gastric cancer (Review). *Exp Ther Med* 2021; **22**: 769 [PMID: 34055068 DOI: 10.3892/etm.2021.10201]
20 **Chen J**, Liu Z, Gao G, Mo Y, Zhou H, Huang W, Wu L, He X, Ding J, Luo C, Long H, Feng J, Sun Y, Guan X. Efficacy of circulating microRNA-130b and blood routine parameters in the early diagnosis of gastric cancer. *Oncol Lett* 2021; **22**: 725 [PMID: 34429765 DOI: 10.3892/ol.2021.12986]
21 **Wang H**, Li J. A systematic review and meta-analysis protocol of clinical characteristics and prognostic significance of mammalian target of rapamycin for gastric cancer patients. *Medicine (Baltimore)* 2020; **99**: e21138 [PMID: 32769866 DOI: 10.1097/MD.0000000000021138]
22 **Shafabakhsh R**, Yousefi B, Asemi Z, Nikfar B, Mansournia MA, Hallajzadeh J. Chitosan: A compound for drug delivery system in gastric cancer-a review. *Carbohydr Polym* 2020; **242**: 116403 [PMID: 32564837 DOI: 10.1016/j.carbpol.2020.116403]
23 **Tan Z**. Recent Advances in the Surgical Treatment of Advanced Gastric Cancer: A Review. *Med Sci Monit* 2019; **25**: 3537-3541 [PMID:

31080234 DOI: 10.12659/MSM.916475]
24 **Zou WB**, Yang F, Li ZS. [How to improve the diagnosis rate of early gastric cancer in China]. *Zhejiang Da Xue Xue Bao Yi Xue Ban* 2015; **44**: 9-14 [PMID: 25851969 DOI: 10.3785/j.issn.1008-9292.2015.01.002]
25 **Mu YP**, Sun WJ, Lu CW, Su XL. MicroRNAs May Serve as Emerging Molecular Biomarkers for Diagnosis and Prognostic Assessment or as Targets for Therapy in Gastric Cancer. *Asian Pac J Cancer Prev* 2015; **16**: 4813-4820 [PMID: 26163596 DOI: 10.7314/apjcp.2015.16.12.4813]
26 **Zheng G**, Xiong Y, Xu W, Wang Y, Chen F, Wang Z, Yan Z. A two-microRNA signature as a potential biomarker for early gastric cancer. *Oncol Lett* 2014; **7**: 679-684 [PMID: 24527072 DOI: 10.3892/ol.2014.1797]
27 **Xiang Z**, Zhou X, Mranda GM, Xue Y, Wang Y, Wei T, Liu J, Ding Y. Identification of the ferroptosis-related ceRNA network related to prognosis and tumor immunity for gastric cancer. *Aging (Albany NY)* 2022; **14**: 5768-5782 [PMID: 35835721 DOI: 10.18632/aging.204176]
28 **White JR**, Banks M. Identifying the pre-malignant stomach: from guidelines to practice. *Transl Gastroenterol Hepatol* 2022; **7**: 8 [PMID: 35243117 DOI: 10.21037/tgh.2020.03.03]
29 **Sukri A**, Hanafiah A, Kosai NR. The Roles of Immune Cells in Gastric Cancer: Anti-Cancer or Pro-Cancer? *Cancers (Basel)* 2022; **14** [PMID: 36010915 DOI: 10.3390/cancers14163922]
30 **Niu X**, Ren L, Hu A, Zhang S, Qi H. Identification of Potential Diagnostic and Prognostic Biomarkers for Gastric Cancer Based on Bioinformatic Analysis. *Front Genet* 2022; **13**: 862105 [PMID: 35368700 DOI: 10.3389/fgene.2022.862105]
31 **Koopaie M**, Ghafourian M, Manifar S, Younespour S, Davoudi M, Kolahdooz S, Shirkhoda M. Evaluation of CSTB and DMBT1 expression in saliva of gastric cancer patients and controls. *BMC Cancer* 2022; **22**: 473 [PMID: 35488257 DOI: 10.1186/s12885-022-09570-9]
32 **Hassen G**, Kasar A, Jain N, Berry S, Dave J, Zouetr M, Priyanka Ganapathiraju VLN, Kurapati T, Oshai S, Saad M, Pathan J, Kamat S, Tirupathi R, Patel UK, Rana RK. Programmed Death-Ligand 1 (PD-L1) Positivity and Factors Associated with Poor Prognosis in Patients with Gastric Cancer: An Umbrella Meta-Analysis. *Cureus* 2022; **14**: e23845 [PMID: 35530821 DOI: 10.7759/cureus.23845]
33 **Waddingham W**, Nieuwenburg SAV, Carlson S, Rodriguez-Justo M, Spaander M, Kuipers EJ, Jansen M, Graham DG, Banks M. Recent advances in the detection and management of early gastric cancer and its precursors. *Frontline Gastroenterol* 2021; **12**: 322-331 [PMID: 34249318 DOI: 10.1136/flgastro-2018-101089]
34 **Feng H**, Liu X. Interaction between ACOT7 and LncRNA NMRAL2P *via* Methylation Regulates Gastric Cancer Progression. *Yonsei Med J* 2020; **61**: 471-481 [PMID: 32469171 DOI: 10.3349/ymj.2020.61.6.471]
35 **Canale M**, Casadei-Gardini A, Ulivi P, Arechederra M, Berasain C, Lollini PL, Fernández-Barrena MG, Avila MA. Epigenetic Mechanisms in Gastric Cancer: Potential New Therapeutic Opportunities. *Int J Mol Sci* 2020; **21** [PMID: 32752096 DOI: 10.3390/ijms21155500]
36 **Negovan A**, Iancu M, Fülöp E, Bănescu C. Helicobacter pylori and cytokine gene variants as predictors of premalignant gastric lesions. *World J Gastroenterol* 2019; **25**: 4105-4124 [PMID: 31435167 DOI: 10.3748/wjg.v25.i30.4105]
37 **Gu X**, Zhang Q, Zhang W, Zhu L. Curcumin inhibits liver metastasis of gastric cancer through reducing circulating tumor cells. *Aging (Albany NY)* 2019; **11**: 1501-1509 [PMID: 30844765 DOI: 10.18632/aging.101848]
38 **Cen D**, Huang H, Yang L, Guo K, Zhang J. Long noncoding RNA STXBP5-AS1 inhibits cell proliferation, migration, and invasion through inhibiting the PI3K/AKT signaling pathway in gastric cancer cells. *Onco Targets Ther* 2019; **12**: 1929-1936 [PMID: 30881044 DOI: 10.2147/OTT.S194463]
39 **Banks M**, Graham D, Jansen M, Gotoda T, Coda S, di Pietro M, Uedo N, Bhandari P, Pritchard DM, Kuipers EJ, Rodriguez-Justo M, Novelli MR, Ragunath K, Shepherd N, Dinis-Ribeiro M. British Society of Gastroenterology guidelines on the diagnosis and management of patients at risk of gastric adenocarcinoma. *Gut* 2019; **68**: 1545-1575 [PMID: 31278206 DOI: 10.1136/gutjnl-2018-318126]
40 **Yang J**, Bo L, Han T, Ding D, Nie M, Yin K. Pathway- and clinical-factor-based risk model predicts the prognosis of patients with gastric cancer. *Mol Med Rep* 2018; **17**: 6345-6356 [PMID: 29532879 DOI: 10.3892/mmr.2018.8722]
41 **Zhang Z**, Wu H, Chong W, Shang L, Jing C, Li L. Liquid biopsy in gastric cancer: predictive and prognostic biomarkers. *Cell Death Dis* 2022; **13**: 903 [PMID: 36302755 DOI: 10.1038/s41419-022-05350-2]
42 **Jin X**, Liu Z, Yang D, Yin K, Chang X. Recent Progress and Future Perspectives of Immunotherapy in Advanced Gastric Cancer. *Front Immunol* 2022; **13**: 948647 [PMID: 35844558 DOI: 10.3389/fimmu.2022.948647]
43 **Ajani JA**, D'Amico TA, Bentrem DJ, Chao J, Cooke D, Corvera C, Das P, Enzinger PC, Enzler T, Fanta P, Farjah F, Gerdes H, Gibson MK, Hochwald S, Hofstetter WL, Ilson DH, Keswani RN, Kim S, Kleinberg LR, Klempner SJ, Lacy J, Ly QP, Matkowskyj KA, McNamara M, Mulcahy MF, Outlaw D, Park H, Perry KA, Pimiento J, Poultsides GA, Reznik S, Roses RE, Strong VE, Su S, Wang HL, Wiesner G, Willett CG, Yakoub D, Yoon H, McMillian N, Pluchino LA. Gastric Cancer, Version 2.2022, NCCN Clinical Practice Guidelines in Oncology. *J Natl Compr Canc Netw* 2022; **20**: 167-192 [PMID: 35130500 DOI: 10.6004/jnccn.2022.0008]
44 **Necula L**, Matei L, Dragu D, Neagu AI, Mambet C, Nedeianu S, Bleotu C, Diaconu CC, Chivu-Economescu M. Recent advances in gastric cancer early diagnosis. *World J Gastroenterol* 2019; **25**: 2029-2044 [PMID: 31114131 DOI: 10.3748/wjg.v25.i17.2029]
45 **Coutzac C**, Pernot S, Chaput N, Zaanan A. Immunotherapy in advanced gastric cancer, is it the future? *Crit Rev Oncol Hematol* 2019; **133**: 25-32 [PMID: 30661655 DOI: 10.1016/j.critrevonc.2018.10.007]
46 **Ratti M**, Lampis A, Hahne JC, Passalacqua R, Valeri N. Microsatellite instability in gastric cancer: molecular bases, clinical perspectives, and new treatment approaches. *Cell Mol Life Sci* 2018; **75**: 4151-4162 [PMID: 30173350 DOI: 10.1007/s00018-018-2906-9]
47 **Alessandrini L**, Manchi M, De Re V, Dolcetti R, Canzonieri V. Proposed Molecular and miRNA Classification of Gastric Cancer. *Int J Mol Sci* 2018; **19** [PMID: 29882766 DOI: 10.3390/ijms19061683]
48 **Massarrat S**, Stolte M. Development of gastric cancer and its prevention. *Arch Iran Med* 2014; **17**: 514-520 [PMID: 24979566]
49 **Song S**, Shu P. Expression of ferroptosis-related gene correlates with immune microenvironment and predicts prognosis in gastric cancer. *Sci Rep* 2022; **12**: 8785 [PMID: 35610340 DOI: 10.1038/s41598-022-12800-6]
50 **Ouyang S**, Li H, Lou L, Huang Q, Zhang Z, Mo J, Li M, Lu J, Zhu K, Chu Y, Ding W, Zhu J, Lin Z, Zhong L, Wang J, Yue P, Turkson J, Liu P, Wang Y, Zhang X. Inhibition of STAT3-ferroptosis negative regulatory axis suppresses tumor growth and alleviates chemoresistance in gastric cancer. *Redox Biol* 2022; **52**: 102317 [PMID: 35483272 DOI: 10.1016/j.redox.2022.102317]
51 **Yao F**, Zhan Y, Pu Z, Lu Y, Chen J, Deng J, Wu Z, Chen B, Tian K, Ni Y, Mou L. LncRNAs Target Ferroptosis-Related Genes and Impair Activation of CD4(+) T Cell in Gastric Cancer. *Front Cell Dev Biol* 2021; **9**: 797339 [PMID: 34966745 DOI: 10.3389/fcell.2021.797339]
52 **Xiao S**, Liu X, Yuan L, Wang F. A Ferroptosis-Related lncRNAs Signature Predicts Prognosis and Therapeutic Response of Gastric Cancer. *Front Cell Dev Biol* 2021; **9**: 736682 [PMID: 34926441 DOI: 10.3389/fcell.2021.736682]
53 **Huo J**, Wu L, Zang Y. Eight-gene prognostic signature associated with hypoxia and ferroptosis for gastric cancer with general applicability.

Epigenomics 2021; **13**: 875-890 [PMID: 33942671 DOI: 10.2217/epi-2020-0411]

54 **Chen W**, Feng Z, Huang J, Fu P, Xiong J, Cao Y, Liu Y, Tu Y, Li Z, Jie Z, Xiao T. Identification of Ferroptosis-Related Long Noncoding RNA and Construction of a Novel Prognostic Signature for Gastric Cancer. *Dis Markers* 2021; **2021**: 7724997 [PMID: 34394774 DOI: 10.1155/2021/7724997]

55 **Wang J**, Qin D, Tao Z, Wang B, Xie Y, Wang Y, Li B, Cao J, Qiao X, Zhong S, Hu X. Identification of cuproptosis-related subtypes, construction of a prognosis model, and tumor microenvironment landscape in gastric cancer. *Front Immunol* 2022; **13**: 1056932 [PMID: 36479114 DOI: 10.3389/fimmu.2022.1056932]

56 **Song X**, Hou L, Zhao Y, Guan Q, Li Z. Metal-dependent programmed cell death-related lncRNA prognostic signatures and natural drug sensitivity prediction for gastric cancer. *Front Pharmacol* 2022; **13**: 1039499 [PMID: 36339625 DOI: 10.3389/fphar.2022.1039499]

57 **Nie H**, Wang H, Zhang M, Ning Y, Chen X, Zhang Z, Hu X, Zhao Q, Chen P, Fang J, Wang F. Comprehensive analysis of cuproptosis-related genes in prognosis, tumor microenvironment infiltration, and immunotherapy response in gastric cancer. *J Cancer Res Clin Oncol* 2023; **149**: 5453-5468 [PMID: 36462036 DOI: 10.1007/s00432-022-04474-4]

58 **Huang J**, Chen M, Pei W, Xu Z, Ning J, Chen C. Distinct tumor microenvironment landscapes in gastric cancer classified by cuproptosis-related lncRNAs. *J Cancer* 2022; **13**: 3687-3700 [PMID: 36606199 DOI: 10.7150/jca.79640]

59 **Liu X**, Nie L, Zhang Y, Yan Y, Wang C, Colic M, Olszewski K, Horbath A, Chen X, Lei G, Mao C, Wu S, Zhuang L, Poyurovsky MV, James You M, Hart T, Billadeau DD, Chen J, Gan B. Actin cytoskeleton vulnerability to disulfide stress mediates disulfidptosis. *Nat Cell Biol* 2023; **25**: 404-414 [PMID: 36747082 DOI: 10.1038/s41556-023-01091-2]

60 **Tomczak K**, Czerwińska P, Wiznerowicz M. The Cancer Genome Atlas (TCGA): an immeasurable source of knowledge. *Contemp Oncol (Pozn)* 2015; **19**: A68-A77 [PMID: 25691825 DOI: 10.5114/wo.2014.47136]

61 **Barrett T**, Wilhite SE, Ledoux P, Evangelista C, Kim IF, Tomashevsky M, Marshall KA, Phillippy KH, Sherman PM, Holko M, Yefanov A, Lee H, Zhang N, Robertson CL, Serova N, Davis S, Soboleva A. NCBI GEO: archive for functional genomics data sets--update. *Nucleic Acids Res* 2013; **41**: D991-D995 [PMID: 23193258 DOI: 10.1093/nar/gks1193]

62 **Addeo A**, Friedlaender A, Banna GL, Weiss GJ. TMB or not TMB as a biomarker: That is the question. *Crit Rev Oncol Hematol* 2021; **163**: 103374 [PMID: 34087341 DOI: 10.1016/j.critrevonc.2021.103374]

63 **Liu L**, Bai X, Wang J, Tang XR, Wu DH, Du SS, Du XJ, Zhang YW, Zhu HB, Fang Y, Guo ZQ, Zeng Q, Guo XJ, Liu Z, Dong ZY. Combination of TMB and CNA Stratifies Prognostic and Predictive Responses to Immunotherapy Across Metastatic Cancer. *Clin Cancer Res* 2019; **25**: 7413-7423 [PMID: 31515453 DOI: 10.1158/1078-0432.CCR-19-0558]

64 **Gene Ontology Consortium**. Gene Ontology Consortium: going forward. *Nucleic Acids Res* 2015; **43**: D1049-D1056 [PMID: 25428369 DOI: 10.1093/nar/gku1179]

65 **Kanehisa M**, Goto S. KEGG: kyoto encyclopedia of genes and genomes. *Nucleic Acids Res* 2000; **28**: 27-30 [PMID: 10592173 DOI: 10.1093/nar/28.1.27]

66 **Tao W**, Li Y, Zhu M, Li C, Li P. LncRNA NORAD Promotes Proliferation And Inhibits Apoptosis Of Gastric Cancer By Regulating miR-214/Akt/mTOR Axis. *Onco Targets Ther* 2019; **12**: 8841-8851 [PMID: 31802897 DOI: 10.2147/OTT.S216862]

67 **Sung H**, Hu N, Yang HH, Giffen CA, Zhu B, Song L, Su H, Wang C, Parisi DM, Goldstein AM, Taylor PR, Hyland PL. Association of high-evidence gastric cancer susceptibility loci and somatic gene expression levels with survival. *Carcinogenesis* 2017; **38**: 1119-1128 [PMID: 29028942 DOI: 10.1093/carcin/bgx090]

68 **Tan Y**, Li Y, Zhu H, Wu X, Mei K, Li P, Yang Q. miR-187/PDLIM1 Gets Involved in Gastric Cancer Progression and Cisplatin Sensitivity of Cisplatin by Mediating the Hippo-YAP Signaling Pathway. *J Oncol* 2022; **2022**: 5456016 [PMID: 36164345 DOI: 10.1155/2022/5456016]

69 **Sun GG**, Sheng SH, Jing SW, Hu WN. An antiproliferative gene FLNA regulates migration and invasion of gastric carcinoma cell in vitro and its clinical significance. *Tumour Biol* 2014; **35**: 2641-2648 [PMID: 24241900 DOI: 10.1007/s13277-013-1347-1]

70 **Liu L**, Chen C, Liu P, Li J, Pang Z, Zhu J, Lin Z, Zhou H, Xie Y, Lan T, Chen ZS, Zeng Z, Fang W. MYH10 Combines with MYH9 to Recruit USP45 by Deubiquitinating Snail and Promotes Serous Ovarian Cancer Carcinogenesis, Progression, and Cisplatin Resistance. *Adv Sci (Weinh)* 2023; **10**: e2203423 [PMID: 36929633 DOI: 10.1002/advs.202203423]

71 **Yu J**, Liang QY, Wang J, Cheng Y, Wang S, Poon TC, Go MY, Tao Q, Chang Z, Sung JJ. Zinc-finger protein 331, a novel putative tumor suppressor, suppresses growth and invasiveness of gastric cancer. *Oncogene* 2013; **32**: 307-317 [PMID: 22370639 DOI: 10.1038/onc.2012.54]

72 **Vierthaler M**, Sun Q, Wang Y, Steinfass T, Poelchen J, Hielscher T, Novak D, Umansky V, Utikal J. ADCK2 Knockdown Affects the Migration of Melanoma Cells *via* MYL6. *Cancers (Basel)* 2022; **14** [PMID: 35205819 DOI: 10.3390/cancers14041071]

73 **Kato S**, Shiozaki A, Kudou M, Shimizu H, Kosuga T, Ohashi T, Arita T, Konishi H, Komatsu S, Kubota T, Fujiwara H, Okamoto K, Kishimoto M, Konishi E, Otsuji E. TRPV2 Promotes Cell Migration and Invasion in Gastric Cancer *via* the Transforming Growth Factor-β Signaling Pathway. *Ann Surg Oncol* 2022; **29**: 2944-2956 [PMID: 34855064 DOI: 10.1245/s10434-021-11132-5]

74 **Jiang H**, Ma P, Duan Z, Liu Y, Shen S, Mi Y, Fan D. Ginsenoside Rh4 Suppresses Metastasis of Gastric Cancer *via* SIX1-Dependent TGF-β/Smad2/3 Signaling Pathway. *Nutrients* 2022; **14** [PMID: 35458126 DOI: 10.3390/nu14081564]

75 **Zhang X**, Wu J. LINC00665 promotes cell proliferation, invasion, and metastasis by activating the TGF-β pathway in gastric cancer. *Pathol Res Pract* 2021; **224**: 153492 [PMID: 34091388 DOI: 10.1016/j.prp.2021.153492]

76 **Xiong R**, Yin T, Gao JL, Yuan YF. HOXD9 Activates the TGF-β/Smad Signaling Pathway to Promote Gastric Cancer. *Onco Targets Ther* 2020; **13**: 2163-2172 [PMID: 32210582 DOI: 10.2147/OTT.S234829]

77 **Xiong R**, Gao JL, Yin T. G3BP1 activates the TGF-β/Smad signaling pathway to promote gastric cancer. *Onco Targets Ther* 2019; **12**: 7149-7156 [PMID: 31564899 DOI: 10.2147/OTT.S213728]

78 **Tao L**, Yu H, Liang R, Jia R, Wang J, Jiang K, Wang Z. Rev-erbα inhibits proliferation by reducing glycolytic flux and pentose phosphate pathway in human gastric cancer cells. *Oncogenesis* 2019; **8**: 57 [PMID: 31591390 DOI: 10.1038/s41389-019-0168-5]

79 **Xia S**, Ji L, Tang L, Zhang L, Zhang X, Tang Q, Feng Z, Lu L. Proteasome Subunit Alpha Type 7 Promotes Proliferation and Metastasis of Gastric Cancer Through MAPK Signaling Pathway. *Dig Dis Sci* 2022; **67**: 880-891 [PMID: 33721161 DOI: 10.1007/s10620-021-06903-9]

80 **Feng X**, Song Z, Huang Q, Jia J, Zhang L, Zhu M, Qian J. AIM2 Promotes Gastric Cancer Cell Proliferation *via* the MAPK Signaling Pathway. *J Healthc Eng* 2022; **2022**: 8756844 [PMID: 35432843 DOI: 10.1155/2022/8756844]

81 **Xu W**, Zhou B, Wang J, Tang L, Hu Q, Chen H, Zheng J, Yan F. tRNA-Derived Fragment tRF-Glu-TTC-027 Regulates the Progression of Gastric Carcinoma *via* MAPK Signaling Pathway. *Front Oncol* 2021; **11**: 733763 [PMID: 34497772 DOI: 10.3389/fonc.2021.733763]

82 **Wu S**, Chen M, Huang J, Zhang F, Lv Z, Jia Y, Cui YZ, Sun LZ, Wang Y, Tang Y, Verhoeft KR, Li Y, Qin Y, Lin X, Guan XY, Lam KO. ORAI2 Promotes Gastric Cancer Tumorigenicity and Metastasis through PI3K/Akt Signaling and MAPK-Dependent Focal Adhesion

Disassembly. *Cancer Res* 2021; **81**: 986-1000 [PMID: 33310726 DOI: 10.1158/0008-5472.CAN-20-0049]
83 **Wang JF**, Zhao K, Chen YY, Qiu Y, Zhu JH, Li BP, Wang Z, Chen JQ. NKCC1 promotes proliferation, invasion and migration in human gastric cancer cells *via* activation of the MAPK-JNK/EMT signaling pathway. *J Cancer* 2021; **12**: 253-263 [PMID: 33391422 DOI: 10.7150/jca.49709]
84 **Zhang Q**, Wang X, Cao S, Sun Y, He X, Jiang B, Yu Y, Duan J, Qiu F, Kang N. Berberine represses human gastric cancer cell growth in vitro and in vivo by inducing cytostatic autophagy *via* inhibition of MAPK/mTOR/p70S6K and Akt signaling pathways. *Biomed Pharmacother* 2020; **128**: 110245 [PMID: 32454290 DOI: 10.1016/j.biopha.2020.110245]
85 **Xu B**, Li S, Fang Y, Zou Y, Song D, Zhang S, Cai Y. Proprotein Convertase Subtilisin/Kexin Type 9 Promotes Gastric Cancer Metastasis and Suppresses Apoptosis by Facilitating MAPK Signaling Pathway Through HSP70 Up-Regulation. *Front Oncol* 2020; **10**: 609663 [PMID: 33489919 DOI: 10.3389/fonc.2020.609663]
86 **Xiang Z**, Li J, Song S, Wang J, Cai W, Hu W, Ji J, Zhu Z, Zang L, Yan R, Yu Y. A positive feedback between IDO1 metabolite and COL12A1 *via* MAPK pathway to promote gastric cancer metastasis. *J Exp Clin Cancer Res* 2019; **38**: 314 [PMID: 31315643 DOI: 10.1186/s13046-019-1318-5]
87 **Du F**, Sun L, Chu Y, Li T, Lei C, Wang X, Jiang M, Min Y, Lu Y, Zhao X, Nie Y, Fan D. DDIT4 promotes gastric cancer proliferation and tumorigenesis through the p53 and MAPK pathways. *Cancer Commun (Lond)* 2018; **38**: 45 [PMID: 29976242 DOI: 10.1186/s40880-018-0315-y]
88 **Peng Y**, Xu Y, Zhang X, Deng S, Yuan Y, Luo X, Hossain MT, Zhu X, Du K, Hu F, Chen Y, Chang S, Feng X, Fan X, Ashktorab H, Smoot D, Meltzer SJ, Hou G, Wei Y, Li S, Qin Y, Jin Z. A novel protein AXIN1-295aa encoded by circAXIN1 activates the Wnt/β-catenin signaling pathway to promote gastric cancer progression. *Mol Cancer* 2021; **20**: 158 [PMID: 34863211 DOI: 10.1186/s12943-021-01457-w]
89 **Liu H**, Fredimoses M, Niu P, Liu T, Qiao Y, Tian X, Chen X, Kim DJ, Li X, Liu K, Dong Z. EPRS/GluRS promotes gastric cancer development *via* WNT/GSK-3β/β-catenin signaling pathway. *Gastric Cancer* 2021; **24**: 1021-1036 [PMID: 33740160 DOI: 10.1007/s10120-021-01180-x]
90 **Li H**, Zhao J, Sun J, Tian C, Jiang Q, Ding C, Gan Q, Shu P, Wang X, Qin J, Sun Y. Demethylation of the SFRP4 Promoter Drives Gastric Cancer Progression *via* the Wnt Pathway. *Mol Cancer Res* 2021; **19**: 1454-1464 [PMID: 34016745 DOI: 10.1158/1541-7786.MCR-20-0933]
91 **Guo Q**, Xu J, Huang Z, Yao Q, Chen F, Liu H, Zhang Z, Lin J. ADMA mediates gastric cancer cell migration and invasion *via* Wnt/β-catenin signaling pathway. *Clin Transl Oncol* 2021; **23**: 325-334 [PMID: 32607811 DOI: 10.1007/s12094-020-02422-7]
92 **Tian S**, Peng P, Li J, Deng H, Zhan N, Zeng Z, Dong W. SERPINH1 regulates EMT and gastric cancer metastasis *via* the Wnt/β-catenin signaling pathway. *Aging (Albany NY)* 2020; **12**: 3574-3593 [PMID: 32091407 DOI: 10.18632/aging.102831]
93 **Yue B**, Liu C, Sun H, Liu M, Song C, Cui R, Qiu S, Zhong M. A Positive Feed-Forward Loop between LncRNA-CYTOR and Wnt/β-Catenin Signaling Promotes Metastasis of Colon Cancer. *Mol Ther* 2018; **26**: 1287-1298 [PMID: 29606502 DOI: 10.1016/j.ymthe.2018.02.024]
94 **Yang XZ**, Cheng TT, He QJ, Lei ZY, Chi J, Tang Z, Liao QX, Zhang H, Zeng LS, Cui SZ. LINC01133 as ceRNA inhibits gastric cancer progression by sponging miR-106a-3p to regulate APC expression and the Wnt/β-catenin pathway. *Mol Cancer* 2018; **17**: 126 [PMID: 30134915 DOI: 10.1186/s12943-018-0874-1]
95 **Xiaobin C**, Zhaojun X, Tao L, Tianzeng D, Xuemei H, Fan Z, Chunyin H, Jianqiang H, Chen L. Analysis of Related Risk Factors and Prognostic Factors of Gastric Cancer with Bone Metastasis: A SEER-Based Study. *J Immunol Res* 2022; **2022**: 3251051 [PMID: 35211630 DOI: 10.1155/2022/3251051]
96 **Song L**, Wang S, Li Q, Lu Y, Yang R, Feng X. Identification and Validation of a m5C RNA Modification-Related Gene Signature for Predicting Prognosis and Immunotherapeutic Efficiency of Gastric Cancer. *J Oncol* 2023; **2023**: 9931419 [PMID: 36936373 DOI: 10.1155/2023/9931419]
97 **Khan M**, Lin J, Wang B, Chen C, Huang Z, Tian Y, Yuan Y, Bu J. A novel necroptosis-related gene index for predicting prognosis and a cold tumor immune microenvironment in stomach adenocarcinoma. *Front Immunol* 2022; **13**: 968165 [PMID: 36389725 DOI: 10.3389/fimmu.2022.968165]
98 **Huo J**, Guan G, Cai J, Wu L. Integrated analysis of 1804 samples of six centers to construct and validate a robust immune-related prognostic signature associated with stromal cell abundance in tumor microenvironment for gastric cancer. *World J Surg Oncol* 2022; **20**: 4 [PMID: 34983559 DOI: 10.1186/s12957-021-02485-y]
99 **Dong R**, Chen S, Lu F, Zheng N, Peng G, Li Y, Yang P, Wen H, Qiu Q, Wang Y, Wu H, Liu M. Models for Predicting Response to Immunotherapy and Prognosis in Patients with Gastric Cancer: DNA Damage Response Genes. *Biomed Res Int* 2022; **2022**: 4909544 [PMID: 36578802 DOI: 10.1155/2022/4909544]
100 **Sun Q**, Guo D, Li S, Xu Y, Jiang M, Li Y, Duan H, Zhuo W, Liu W, Zhu S, Wang L, Zhou T. Combining gene expression signature with clinical features for survival stratification of gastric cancer. *Genomics* 2021; **113**: 2683-2694 [PMID: 34129933 DOI: 10.1016/j.ygeno.2021.06.018]
101 **Huo J**, Wu L, Zang Y. Construction and Validation of a Universal Applicable Prognostic Signature for Gastric Cancer Based on Seven Immune-Related Gene Correlated With Tumor Associated Macrophages. *Front Oncol* 2021; **11**: 635324 [PMID: 34178625 DOI: 10.3389/fonc.2021.635324]
102 **Guo X**, Liang X, Wang Y, Cheng A, Zhang H, Qin C, Wang Z. Significance of Tumor Mutation Burden Combined With Immune Infiltrates in the Progression and Prognosis of Advanced Gastric Cancer. *Front Genet* 2021; **12**: 642608 [PMID: 34306002 DOI: 10.3389/fgene.2021.642608]
103 **Hu C**, Zhou Y, Liu C, Kang Y. A novel scoring system for gastric cancer risk assessment based on the expression of three CLIP4 DNA methylation-associated genes. *Int J Oncol* 2018; **53**: 633-643 [PMID: 29901187 DOI: 10.3892/ijo.2018.4433]
104 **Huang J**, Song J, Li X, Liu S, Huang W, Shen Z, Cheng Y, Kou S, Gao Z, Tian Y, Hu J. Analysis and prognostic significance of tumour immune infiltrates and immune microenvironment of m6A-related lncRNAs in patients with gastric cancer. *BMC Med Genomics* 2022; **15**: 164 [PMID: 35879790 DOI: 10.1186/s12920-022-01318-5]
105 **Zhao Y**, Hu S, Zhang J, Cai Z, Wang S, Liu M, Dai J, Gao Y. Glucoside xylosyltransferase 2 as a diagnostic and prognostic marker in gastric cancer *via* comprehensive analysis. *Bioengineered* 2021; **12**: 5641-5654 [PMID: 34506251 DOI: 10.1080/21655979.2021.1967067]
106 **Cao L**, Wang S, Zhang Y, Wong KC, Nakatsu G, Wang X, Wong S, Ji J, Yu J. Zinc-finger protein 471 suppresses gastric cancer through transcriptionally repressing downstream oncogenic PLS3 and TFAP2A. *Oncogene* 2018; **37**: 3601-3616 [PMID: 29610526 DOI: 10.1038/s41388-018-0220-5]
107 **Yang Y**, Shi Z, Bai R, Hu W. Heterogeneity of MSI-H gastric cancer identifies a subtype with worse survival. *J Med Genet* 2021; **58**: 12-19 [PMID: 32170001 DOI: 10.1136/jmedgenet-2019-106609]

108 **Pietrantonio F**, Randon G, Di Bartolomeo M, Luciani A, Chao J, Smyth EC, Petrelli F. Predictive role of microsatellite instability for PD-1 blockade in patients with advanced gastric cancer: a meta-analysis of randomized clinical trials. *ESMO Open* 2021; **6**: 100036 [PMID: 33460964 DOI: 10.1016/j.esmoop.2020.100036]

109 **Kwon M**, An M, Klempner SJ, Lee H, Kim KM, Sa JK, Cho HJ, Hong JY, Lee T, Min YW, Kim TJ, Min BH, Park WY, Kang WK, Kim KT, Kim ST, Lee J. Determinants of Response and Intrinsic Resistance to PD-1 Blockade in Microsatellite Instability-High Gastric Cancer. *Cancer Discov* 2021; **11**: 2168-2185 [PMID: 33846173 DOI: 10.1158/2159-8290.CD-21-0219]

110 **Chao J**, Fuchs CS, Shitara K, Tabernero J, Muro K, Van Cutsem E, Bang YJ, De Vita F, Landers G, Yen CJ, Chau I, Elme A, Lee J, Özgüroglu M, Catenacci D, Yoon HH, Chen E, Adelberg D, Shih CS, Shah S, Bhagia P, Wainberg ZA. Assessment of Pembrolizumab Therapy for the Treatment of Microsatellite Instability-High Gastric or Gastroesophageal Junction Cancer Among Patients in the KEYNOTE-059, KEYNOTE-061, and KEYNOTE-062 Clinical Trials. *JAMA Oncol* 2021; **7**: 895-902 [PMID: 33792646 DOI: 10.1001/jamaoncol.2021.0275]

111 **Pietrantonio F**, Miceli R, Raimondi A, Kim YW, Kang WK, Langley RE, Choi YY, Kim KM, Nankivell MG, Morano F, Wotherspoon A, Valeri N, Kook MC, An JY, Grabsch HI, Fucà G, Noh SH, Sohn TS, Kim S, Di Bartolomeo M, Cunningham D, Lee J, Cheong JH, Smyth EC. Individual Patient Data Meta-Analysis of the Value of Microsatellite Instability As a Biomarker in Gastric Cancer. *J Clin Oncol* 2019; **37**: 3392-3400 [PMID: 31513484 DOI: 10.1200/JCO.19.01124]

112 **Ajani JA**, Jiang Y, Faust J, Chang BB, Ho L, Yao JC, Rousey S, Dakhil S, Cherny RC, Craig C, Bleyer A. A multi-center phase II study of sequential paclitaxel and bryostatin-1 (NSC 339555) in patients with untreated, advanced gastric or gastroesophageal junction adenocarcinoma. *Invest New Drugs* 2006; **24**: 353-357 [PMID: 16683077 DOI: 10.1007/s10637-006-6452-1]

113 **Tseng LL**, Cheng HH, Yeh TS, Huang SC, Syu YY, Chuu CP, Yuh CH, Kung HJ, Wang WC. Targeting the histone demethylase PHF8-mediated PKCα-Src-PTEN axis in HER2-negative gastric cancer. *Proc Natl Acad Sci U S A* 2020; **117**: 24859-24866 [PMID: 32958674 DOI: 10.1073/pnas.1919766117]

Published by **Baishideng Publishing Group Inc**
7041 Koll Center Parkway, Suite 160, Pleasanton, CA 94566, USA
Telephone: +1-925-3991568
E-mail: bpgoffice@wjgnet.com
Help Desk: https://www.f6publishing.com/helpdesk
https://www.wjgnet.com